Fossil Record 29 (1) 2026, 115–133 | DOI 10.3897/fr.29.175525

PENSOFT

für Natur MUSEUM FÜR NATURKUNDE BERLIN

The oldest Jurassic anurans from continental Africa (Tendaguru Hill, Tanzania)

Alfred J. A. Lemierre[1], Wolf-Dieter Heinrich[2], David C. Blackburn[3]

1 *Royal Tyrrell Museum of Palaeontology, Box 7500 Drumheller, Alberta, T0J 0Y0, Canada*

2 *Museum für Naturkunde, Leibniz-Institut für Evolutions- und Biodiversitätsforschung, Invalidenstraße 43, 10115 Berlin, Germany*

3 *Department of Natural History, 1659 Museum Road, Florida Museum of Natural History, University of Florida, Gainesville, Florida, 32611, USA*

https://zoobank.org/7DC4BF45-D42A-4BA9-B6DC-6083EB5E7764

Corresponding author: Alfred J. A. Lemierre (alfred.lemierre@gov.ab.ca)

Academic editor: Florian Witzmann ♦ **Received** 20 October 2025 ♦ **Accepted** 26 February 2026 ♦ **Published** 19 March 2026

Abstract

Anurans are a diverse clade of tetrapods with a rich evolutionary history beginning ~250 Ma. Most time-calibrated molecular phylogenetic analyses place the early diversification of anurans during the Jurassic, with the emergence of several major modern anuran clades linked to the break-up of the Pangea. However, remains of crown-anurans before the Cretaceous are scarce, especially in Gondwana. Here, we described the first lissamphibian specimens from Jurassic outcrops in continental sub-Saharan Africa, with five specimens from the Jurassic Middle Dinosaur Member of the Tendaguru Formation (Tendaguru Hill, Tanzania). The specimens represent at least two distinct lissamphibian taxa, based on humeral morphologies. Comparisons with humeri from other lissamphibian clades reveal that the morphology of the Tendaguru specimens fits within Salientia (stem-Anura). Further, two humeri can be securely assigned to Anura, making these the oldest occurrence of the crown-group in Africa as well as within Gondwana.

Key Words

Africa, biogeography, frogs, Gondwana, Lissamphibia, Salientia

Introduction

Anura (frogs and toads) is today one of the most diverse tetrapod clades, surpassed in number of species only by Squamata and Aves (Frost 2025). The > 7,900 living species of anurans are found in habitats ranging from tropical forests to deserts and on all continents except Antarctica, where Eocene fossils reveal their past presence (Mörs et al. 2020). Anurans have a rich and long evolutionary history, extending to at least 250 Mya with the salientian (stem-anuran) *Triadobatrachus massinoti* (Piveteau, 1936). Most time-calibrated molecular phylogenetic analyses (e.g., Frazão et al. 2015; Feng et al. 2017; Portik et al. 2023) place the early diversification of anurans in the Jurassic, coinciding with the breakup of Pangea. The 'modern frogs' of the Neobatrachia (representing > 95% of extant species; Frost 2025) likely arose in Gondwana (South America, Australia, Africa, Antarctica, India) with the three major component clades—Hyloidea, Myobatrachoidea, and Ranoidea—corresponding to the isolation of Gondwanan landmasses (South America, Australia, and Africa, respectively) during the Cretaceous and through the early Cenozoic (Feng et al. 2017).

Although South America has yielded important stem-anuran fossils from the Jurassic (Báez and Basso 1996; Báez and Nicoli 2004, 2008, 2025; Barcelos and Santos 2023), none are considered to be stem- or crown-group members of the Neobatrachia (Chen et al. 2016; Wang et al. 2018; Báez and Nicoli 2025). In Africa, amphibians are recorded from three Jurassic localities: salamanders and albanerpetontids from Guelb el Ahmar (Middle Jurassic, Morocco; Haddoumi et al. 2016), unidentified amphibians from Tendaguru Hill (Late Jurassic, Tanzania; Aberhan et al. 2002; Bussert et al. 2009), and albanerpetontids, alytoid and pipimorph anurans from Anoual (Late Jurassic/Early Cretaceous, Morocco; Jones et al. 2003;

Copyright: This is an open access article distributed under the terms of the CC0 Public Domain Dedication.

Gardner and Rage 2016; Lemierre et al. 2023). Though the Tendaguru amphibians might represent anurans and have been known for > 20 years, these fossils have never been illustrated or otherwise described.

Here we describe and illustrate the putative amphibian specimens from the Tendaguru Hill. In total, we describe five specimens, all referable to Lissamphibia. We identify three humeri, compare these to humeri from all major lissamphibian clades, and subsequently confirm that their morphologies correspond to Salientia and its crown-clade Anura. We also compare the two best-preserved humeri to representatives of extant crown-anuran families, as well as several Jurassic and Cretaceous anuran humeri, to determine whether they might be referable to lineages within Anura.

Geological context

Geography, sedimentology, stratigraphy and history of the Tendaguru Formation

The Tendaguru Hill is located in southeastern Tanzania, approximately 60 km northwest of Lindi (Fig. 1; 9°42'0"S, 39°12'0"E). Geologically, this area lies within the southwestern region of the Mandawa Basin (a sub-basin of the Somali Basin), and its formation and evolution are closely associated with rifting and seafloor spreading processes leading to the breakup of Gondwana (e.g., Bussert et al. 2009; Mishra et al. 2022).

Numerous fossiliferous localities have been identifid within the Tendaguru region since the early 20th Century, and these yield some of the best-known African dinosaurs (Maier 2003). The exposed layers are grouped into the Tendaguru Formation, deposited during the Late Jurassic to Early Cretaceous (Middle Oxfordian – Valanginian/Hauterivian; Bussert and Aberhan 2004; Sames 2008; Bussert et al. 2009). The Tendaguru Formation (110 m thick), which discordantly overlies the Proterozoic basement, is comprised of alternating units of fossil-rich marine sandstone and fine-grained dinosaur-bearing coastal and tidal deposits. This cyclic nature of the sedimentary sequence suggests an influence by eustatic sea level changes (Aberhan et al. 2002; Bussert and Aberhan 2004; Bussert et al. 2009; Mishra et al. 2022). The Formation has been divided into six stratigraphic units (Bussert et al. 2009; Hübner et al. 2021; here listed oldest to youngest): (1) Lower Dinosaur Member, (2) *Nerinella* Member, (3) Middle Dinosaur Member, (4) *Indotrigonia africana* Member, (5) Upper Dinosaur Member, and (6) *Rutitrigonia bornhardti-schwarzi* Member.

Since the original German Tendaguru Expedition (1909–1913), the Tendaguru Formation has been primarily known for its rich dinosaur assemblage, including sauropods (e.g., *Dicraeosaurus*, *Giraffatitan*; Janensch 1935; Mannion et al. 2019), theropods (e.g. *Elaphrosaurus*, *Veterupristisaurus*; Janensch 1920; Rauhut 2011) and ornithischians (e.g., *Dysalotosaurus*, *Kentrosaurus*; Janensch 1955; Redelstorff et al. 2013; Hübner et al. 2021). In addition to this diverse dinosaur fauna, additional vertebrates have been identified including amphibians, crocodilians, lizards, pterosaurs, mammals, and fishes (e.g., Heinrich 2003; Heinrich et al. 2001; Aberhan et al. 2002; Bussert et al. 2009). Among these, the most commonly recovered vertebrate is a crocodilian tentatively referred to *Bernissartia* (Heinrich et al. 2002). Fishes are diverse and represented by batoids (e.g., *Engaibatis schultzei*), hybodonts (e.g., *Hybodus* sp.), neoselachians (*Sphenodus* sp.) and neopterygians (e.g., *Lepidotes tendagurensis*; Hennig 1914; Arratia et al. 2002). In addition, a diverse invertebrate fauna (e.g., Aitken 1961; Aberhan et al. 2002; Schudack and Schudack 2002; Sames 2008) and flora (e.g., Kahlert et al. 1999; Schudack 1999; Schrank 2005, 2010) have been recovered from the Tendaguru Formation.

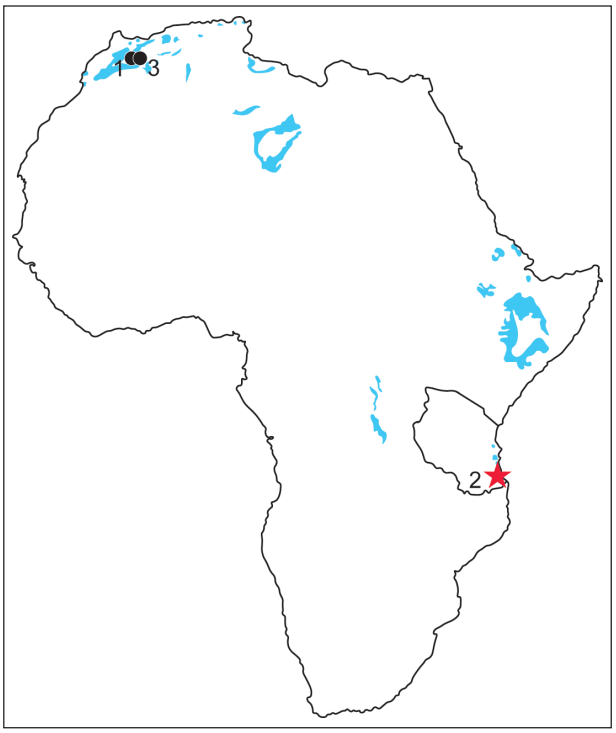

Figure 1. Map of Jurassic African outcrops (in blue) and localities where lissamphibians have been identified. Localities shown are as follows: (1) Guelb el Ahmar (Middle Jurassic; Morocco); (2) Tendaguru Hill (Upper Jurassic; Tanzania); (3) Anoual (Upper Jurassic/ Lower Cretaceous; Morocco). Black outline within Africa represents internationally recognized political borders of Tanzania. Jurassic outcrops are based on the 1:10M-scale geological map of Africa (Thiéblemont, 2016).

Jg/WJ locality

The specimens that we studied derive from acid-prepared matrix (see below) from the locality of Jg/WJ (situated near the village of Kindope, approximately 2.3 km north-northwest of Tendaguru Hill). This locality was extensively excavated during the German Tendaguru Expedition (1909–1913). The layers within locality Jg/WJ have been

correlated to the Middle Dinosaur member (Aberhan et al. 2002; Bussert et al. 2009; Hübner et al. 2021). This member primarily consists of fine-grained deposits, including ripple cross-bedded to cross-laminated calcareous sandstone, and ripple cross-laminated or horizontally bedded siltstone and claystone, tentatively assigned to a Late Kimmeridgian age (Bussert et al. 2009; Hübner et al. 2021).

Within the Middle Dinosaur Member, four distinct bonebeds (BB-1 to BB-4) are intercalated in its middle section (Hübner et al. 2021: 283, Tab. 1, 2; also present within Jg/WJ). These four bonebeds are rich in remains assigned to the ornithopod *Dysalotosaurus lettowvorbecki* (unique to the Tendaguru region) and mainly consist of calcareous medium sandstone to fine-grained sandstone, siltstone, claystone, mud clasts, and reworked caliche nodules (Bussert et al. 2009). The thickness of each bonebed is not precisely known, except for BB-3 (10–30 cm thick; Janensch 1914; Hübner et al. 2021). Additional samples with more precise data from the bonebeds in Jg/WJ could not be recovered during the German Tanzanian Tendaguru Expedition 2000 because the site was covered with substantial overburden (Heinrich et al. 2001).

Palaeoenvironment of the Middle Dinosaur Member and Jg/WJ locality

Available sedimentological and palaeontological evidence from the Middle Dinosaur Member suggests the depositional environment is primarily a shallow marine environment under tidal influence, such as a costal embayment or a wave-protected lagoon (Bussert et al. 2009; Hübner et al. 2021), with nearby low-relief coastal plain with erosional episodes (as highlighted by lag deposits; Bussert et al. 2009; Hübner et al. 2021). There is no evidence of connection with an open sea recovered within the Middle Dinosaur Member (unlike previously proposed, via a large estuary, e.g., Parkinson 1930). Within the Member, ostracod assemblages have been used to identify a regressive trend from the lower to middle sections (the latter in which the bonebeds are intercalated). Hence, a more precise palaeoenvironment of deposition for the Middle Dinosaur Member has been proposed: a sabkha-like coastal plain with brackish lakes and ponds with periodical freshwater influx (Schudack 1999; Aberhan et al. 2002; Schudack and Schudack 2002; Sames 2008; Bussert et al. 2009). The presence of reworked caliche nodules identified within the bonebeds at the Jg/WJ locality has been suggested to be the result of a warm to hot climate with seasonal precipitation (Aberhan et al. 2002). Study of the palaeoflora and palynological analyses have identified that nearby inland (and outside tidal influence) regions were relatively dry, with an araucarian vegetation composed of groups such as podocarpaceans, cycadeans, cheirolepidiaceans, araucarians, ginkgophytes, and pteridosperms (Kahlert et al. 1999; Schrank 2010). In addition, the study of autochthonous palaeoflora has identified bryophytes and pteridophytes that likely formed a dense herbaceous vegetation surrounding the different bodies of water, especially during rainy seasons (Kahlert et al. 1999; Schrank 2010). This vegetated landscape has been suggested to serve as the preferred feeding ground for the various sauropods identified within the Member (as well as for the theropods that preyed upon them, e.g., Aberhan et al. 2002). Thus, the palaeoenvironment of locality of Jg/WJ (and the entire Middle Dinosaur Member) was likely a sabkha-like coastal plain with dense herbaceous vegetation surrounding brackish lakes and ponds that would have occasional freshwater influx under a warm and dry climate with seasonal precipitation.

Materials and methods

The specimens were part of blocks collected in the initial German Tendaguru Expedition between 1910 and 1913 that removed large blocks and shipped them back to the Museum für Naturkunde in Berlin (Maier 2003). Most of the blocks were not labeled with the specific bonebed, and some of the original documentation was lost during World War II (Hübner et al. 2021). As such, only a few blocks can be tentatively matched to individual bonebeds. A single block housing amphibian remains, Jg 931, which can be tentatively assigned to BB-3 (based on available archives). Two specimens discussed here, MB. Am 1554 and 1555, were recovered from Jg 931, and hence can be tentatively assigned to BB-3, while the remaining specimens cannot be assigned to a precise bonebed within the locality Jg/WJ. There has been a focus on documenting the microvertebrate diversity of the Tendaguru Formation since the 1990s, including processing blocks collected in the early 20th century with a formic acid treatment. The residue was screenwashed through 0.5 mm sieves, before sorting under a microscope. The amphibian specimens are currently stored in the vertebrate palaeontology collections of the Museum für Naturkunde, Berlin (Germany) in the collection of fossil amphibians.

CT-scan and 3D model reconstruction

MB.Am. 1551–1555 were subjected to micro-tomographic analysis at the Museum für Naturkunde Berlin (RRID:SCR_022585) using a Phoenix nanotom X-ray|s tube (Waygate Technologies, Wunstorf, Germany; RRID:SCR_022582) at 105–120 kV and 60–100 µA, generating 1440, 3 times averaged, projections with 750 ms per scan. The different kV- and projection-settings depended on the respective specimen size, which is also responsible for the range of the effective voxel size between 1.1–1.8 µm. The cone beam reconstruction was performed using the datos|x 2.2 reconstruction software (Waygate Technologies, Wunstorf, Germany) and the data were visualized in VG Studio Max 3.5 (Volume Graphics GmbH, Heidelberg Germany). In total 901 to

2302 virtual slices were produced for each specimen with a resolution of 01.1–1.82 µm. Each stack of slices was cropped to remove a maximum of empty spaces, and contrast was enhanced. 3D models were produced using the software 3D Slicer (Fedorov et al. 2012) using the threshold function. Each 3D model was exported as an .stl file (Suppl. material 1: table S1). All CT-data and produced 3D models are available on MorphoSource (https://www.morphosource.org/projects/000743624).

We compared our specimens to humeri from extant and extinct lissamphibian taxa belonging to all four lissamphibian clades: Albanerpetontidae (extinct), Gymnophionomorpha (and its crown-clade Gymnophiona), Caudata (and its crown-clade Urodela) and Salientia (and its crown-clade Anura). Comparisons to albanerpetonids, caecilians, and extinct caudates and salientians were made using available figures and descriptions from the literature. In total, we compared our specimens to 43 extinct taxa, from the Early Triassic to the Eocene (see Suppl. material 1: table S2 for a complete list). Comparisons to extant urodeles and anurans were made using available CT-scan and 3D models on MorphoSource (Blackburn et al. 2024). In total, we compare our specimens to humeri of 20 urodele taxa, representing all extant families (Suppl. material 1: table S3, figs S1, S2).

Humeri are often recovered within the anuran fossil record, and several morphologies have been used to diagnostic clades or families (e.g., Rage 1974, 1984, 2016; Sanchíz and Estes 1982; Sanchíz et al. 1993; Otero et al. 2014). However, most humeral morphologies used to identify anuran families are not unique (and often are geographically or temporally restricted in relevance, e.g., Bailon 1999) and have rarely been tested within a phylogenetic context (for notable recent exceptions, se Gómez 2016; Gómez and Turazzini 2021). Furthermore, humeral morphology can be shaped by specific locomotion modes (e.g., forward burrowing; Keeffe and Blackburn 2020) and sexual dimorphism. Although only alytids, neobatrachians, and pipimorphs have been identified within the Mesozoic record of Africa, we compared our humeri to representatives of major anuran clades as well as several Jurassic and Cretaceous anurans of uncertain affinities. In total, we compared our specimens to humeri of 24 non-neobatrachian anuran taxa, representing all major non-neobatrachian clades (Suppl. material 1: table S4, figs S3, S4), and of 126 neobatrachian taxa (Suppl. material 1: table S5, figs S5–S10), representing all recognized families (following Portik et al. 2023, with the addition of the newly recognized Caligophrynidae and Neblinaphrynidae; Fouquet et al. 2024). Our studied data includes a large portion of African neobatrachians, because of their availability in a previous study (Lemierre et al. 2025b).

Institutional abbreviation

CAS:HERP: California Academy of Sciences Herpetology collection (San Francisco, California, USA); **ces:f:** Center for Ecological Science, Indian Institute of Science (Karnataka, India); **KU: KUH:** University of Kansas, Herpetology Collections (Lawrence, USA); **LSUMZ:** Louisiana State University Museum of Zoology (Baton Rouge, USA); **MB. Am:** collection of amphibians; Museum für Naturkunde, Berlin (Germany); **MVZ: Herp:** Museum of Vertebrate Zoology, Collection of amphibians and reptiles at the University of California (Berkeley, USA); **nhmw:** Naturhistorisches Museum Wien, Zoological Department, Vertebrates (Wien, Austria); **NHMUK.ZOO:** Natural History Museum, Zoology collection (London, UK); **UF-Herp:** University of Florida, Herpetology collection (Gainesville, USA); **UMZC:** University Museum of Zoology, Cambridge (Cambridge, UK); **YP-VZ:** Vertebrate Zoology Division – Herpetology, Yale Peabody Museum (New Heaven, USA).

Anatomical nomenclature

Terms proposed to identify features of the salientian humerus vary across the literature, including both latinized and anglicized terms (Table 1). We follow the terminology (Fig. 2) proposed by Keeffe and Blackburn (2020), with some addition from Evans and Borsuk-Białynicka (2009).

Systematic Palaeontology

Lissamphibia Haeckel, 1866
Salientia Laurenti, 1768
Anura Duméril, 1805

Anura indeterminate

Referred specimens. MB.Am. 1551, distal portion of a left humerus; and MB.Am. 1552, distal portion of a right humerus.

Description. ***MB.Am. 1551*:** Only the distal head and the base of the diaphysis are preserved (Fig. 3). The humeral head is well-ossified and large (~72% of distal width; Fig. 2). The lateral and medial margins of the humerus are straight (Fig. 3A). The humeral head is slightly shifted laterally from the diaphyseal axis (Fig. 3). The cubital fossa is not well-delimited, shallow and reduced to a crescent-shaped fossa that abuts the humeral head (Fig. 3A). The epicondyles are asymmetrically developed, with the ulnar more developed than the radial (Fig. 3A–D). The radial epicondyle is reduced, and indistinct in ventral view (i.e., not prominent and pressed against the humeral head; Fig. 3F). The ulnar epicondyle protrudes laterodistally and extends distally along ~85% of and terminating well before the margin of the humeral head (Fig. 3A, D). The olecranon scar is small and triangular-shaped (Fig. 3B).

***MB.Am. 1552*:** As for MB.Am. 1551, only the distal head and base of the diaphysis are preserved (Fig. 3G–L). The diaphysis is straight with the humeral head in line with the diaphyseal axis (Fig. 3G, H). The humeral head is well-ossified and large (~85% of distal width). The cubital

Table 1. Comparison between nomenclatural schemes for features of lissamphibian humeri.

This study	Gaupp 1896	Bolkay 1919	Duellman and Trueb 1986	Sanchíz 1998	Holman 2003	Jenkins et al. 2007	Sigurdsen and Bolt 2009; Sigurdsen et al. 2012	Evans and Borsuk-Białynicka (2009)	Nakamura and Ota 2015	Delfino 2020	Keeffe and Blackburn (2020)
ossified articular cartilage	caput humeri	caput humeri	-	-	calcified cartilaginous head of humerus	humeral head	humeral head	proximal condyle	-	ossified articular cartilage	ossified articular cartilage
tubercule	spina tuberculi medialis	spina tuberculi medialis	-	-	-	tuberosity	dorsal process	-	spina tuberculi medialis	tubercule	tubercule
ventral crest	crista ventralis	crista ventralis	crista ventralis	crista ventralis	ventral crest	deltopectoral crest	deltopectoral crest	ventral crest	crista ventralis	ventral crest	ventral crest
paraventral crest		crista paraventralis	-	crista paraventralis	-	-	-	-	crista paraventralis	-	paraventral crest
medial groove		fossula dividens	-	-	-	-	-	-	fossula dividens	medial groove	medial groove
lateral crest	crista lateralis	crista lateralis	crista lateralis	crista lateralis	-	-	-	-	crista lateralis	-	lateral crest
radial epiconyle	epcondylus lateralis	epcondylus radialis	lateral epicondyle	epcondylus radialis	radial (lateral) epicondyle	ectepicondyle	ectepicondyle	radial epicondyle	epicondylus radialis	radial epiconyle	radial epiconyle
cubital fossa	fossa cubitalis ventralis	fossa cubitalis ventralis	-	fossa cubitalis ventralis	cubital fossa	-	-	ventral cubital fossa	-	-	cubital fossa
medial crest	crista medialis	crista medialis	crista medialis	crista medialis	mesial crest	-	-	-	crista medialis	-	medial crest
ulnar epicondyle	epicondylus medialis	epcondylus ulnaris	-	epcondylus ulnaris	ulnar (medial) epicondyle	entepicondyle	entepicondyle	ulnar epicondyle	epicondylus ulnaris	medial epicondyle	medial epicondyle
humeral head	eminentia capitata	eminentia capitata	-	eminentia capitata	distal condyle	capitulum	capitulum	capitate eminence	emientia capitata	humeral head	humeral head
ulnar trochlea	-	-	-	-	-	trochlea	trochlea	ulnar trochlea	-	-	-
olecranon scar	-	-	-	impressio olecraneana	-	-	-	olecranon scar	olecranon scar	-	-

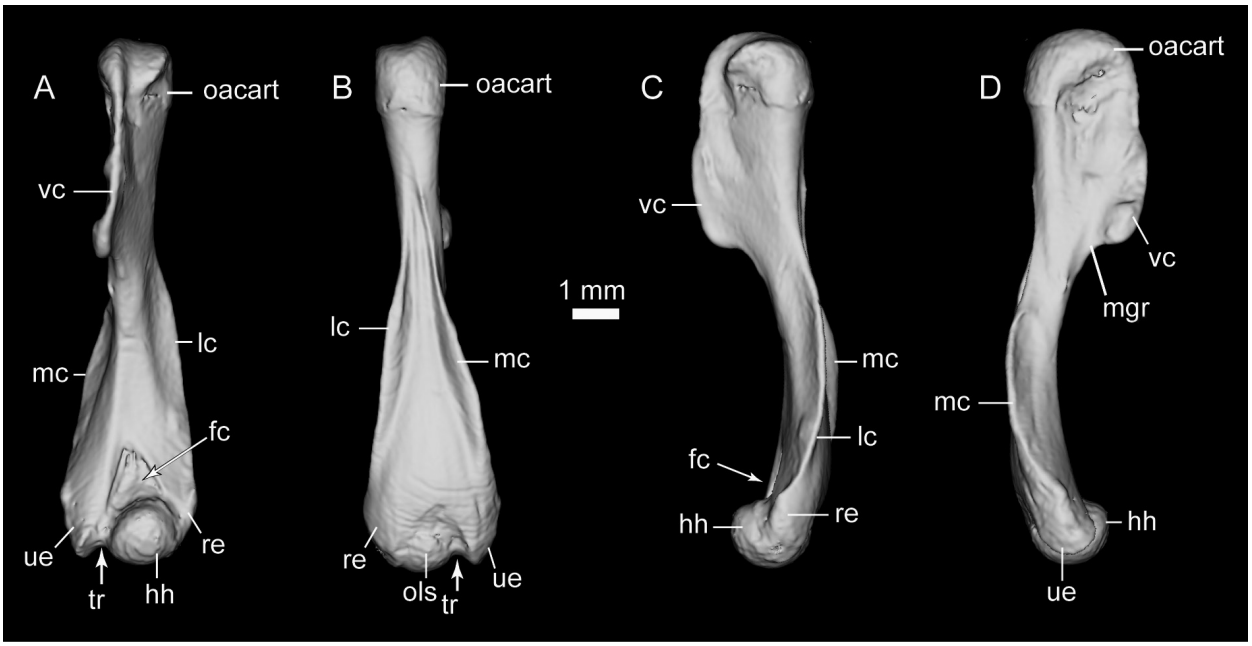

Figure 2. Generalized humeral anatomy for Salientia, based on the left humerus of *Ascaphus truei* (UF:Herp:80664; Ascaphidae, Anura). Left humerus in **A.** Ventral; **B.** Dorsal; **C.** Lateral and **D.** Medial views. Abbreviations: fc, cubital fossa; hh, humeral head; lc, lateral crest; mc, medial crest; mgr, medial grove; oacart, ossified articular cartilage; ols, olecranon scar; re, radial epicondyle; tr, trochlea; ue, ulnar epicondyle; vc, ventral crest.

fossa is not well-delimited, shallow and crescent-shaped (Fig. 3G). Epicondyles are asymmetrically developed, with the ulnar epicondyle more developed (Fig. 3G–J). The radial epicondyle is reduced and indistinct from the humeral head in ventral view (Fig. 3G). The ulnar epicondyle extends distally along ~85% of the humeral head and protrudes distomedially (Fig. 3G, H). The olecranon scar is small and triangular-shaped (Fig. 3H).

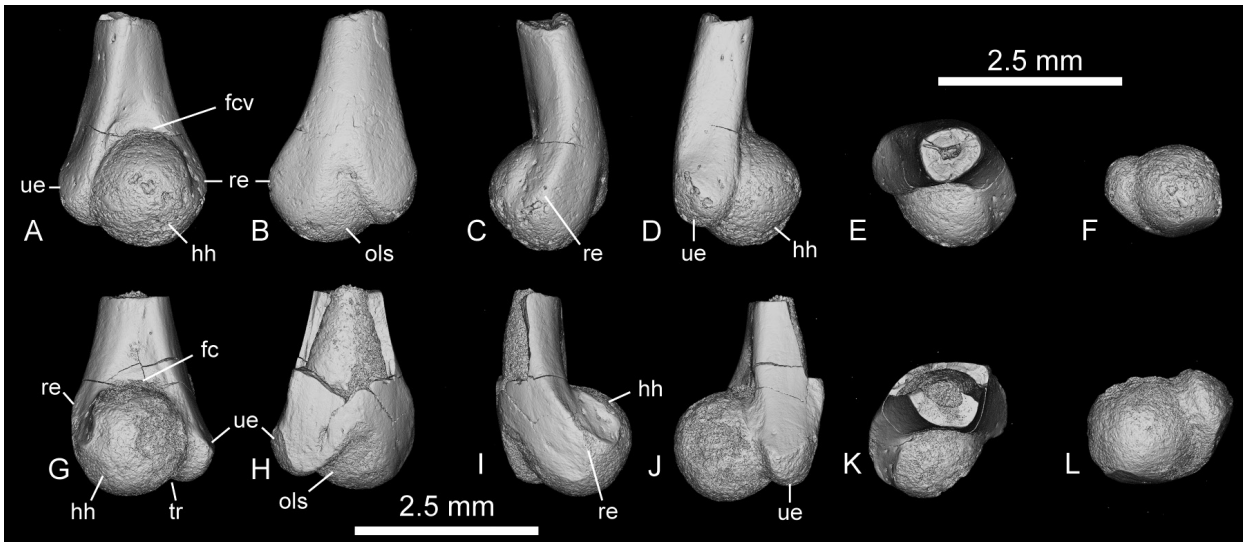

Figure 3. Indeterminate anurans of the Tendaguru Formation. **A–F.** MB. Am 1551, Anura indet., distal portion of a left humerus in **A.** Ventral; **B.** Dorsal; **C.** Lateral; **D.** Medial; **E.** Proximal and **F.** Distal views; **G–L.** MB. Am 1552, Anura indet., distal portion of a right humerus in **G.** Ventral; **H.** Dorsal; **I.** Lateral; **J.** Medial; **K.** Proximal and **L.** Distal views. Abbreviations: fc, cubital fossa; hh, humeral head; lc, lateral crest; mc, medial crest; ols, olecranon scar; re, radial epicondyle; tr, trochlea; ue, ulnar epicondyle.

Salientia indeterminate

Referred specimens. MB.Am. 1553, diaphysis and part of the distal portion of a right humerus; MB.Am. 1554, fragment of tibiofibula or radioulna; MB.Am. 1555, phalanx.

Description. ***Humerus*:** MB.Am. 1553 is smaller than the other two humeri and preserves part of a straight slender diaphysis (Fig. 4A–D). No crista ventralis is present. Only the dorsalmost portion of the distal portion of the humerus is preserved. The preserved small portion of the ulnar epicondyle suggests it might have been distinct from the humeral head in ventral view if complete (Fig. 4C), while the shape of the lateral margin of MB. Am. 1553 suggests the radial epicondyle was very reduced. This suggests epicondyles might be asymmetrically developed, but we cannot be certain. The olecranon scar is small, shallow, and triangular (Fig. 4B).

***Limb bone*:** MB.Am. 1554 is a small fragment of either a proximal or distal composite limb bone (Fig. 4E–I). On what we interpret to be the dorsal and ventral surfaces, there is a faint sulcus suggesting the boundary between two fused bones (Fig. 4E, F), as is found in an anuran radioulna or tibiofibula.

***Phalanx*:** MB.Am. 1555 is a small, thin bone that appears to be a phalanx missing its proximal and distal portions (Fig. 4J–M). The diaphysis is slender and elongated.

Discussion

How many lissamphibians in the Tendaguru Formation?

The earliest mention of a lissamphibian within the Tendaguru Formation was by Nopcsa (1930), who described an anuran taxon, *Stremmeia scabra*, based on a pair of fused metapodials. However, this taxon was later recognized as a reptile (Stremme 1916; Hecht 1963; Estes and Reig 1973; Sanchíz 1998). No lissamphibian specimens were identified within the Tendaguru Formation until the Tendaguru Expedition 2000 during which the specimens studied here were recovered (see above; mentioned as ?Salientia in Aberhan et al. 2002).

MB.Am. 1551–1553 all share the following combination of characters (almost) unique to Lissamphibia: (1) a rather slender diaphysis; (2) no humeral foramina (in other tetrapod, an ulnar epicondyle foramen is present; Sigurdsen and Bolt 2009); (3) no ulnar condyle (in most tetrapods, both a radial and ulnar condyles are present, whereas in lissamphibians only the radial condyle, here called humeral head, is present; Sigurdsen and Bolt 2009) and (4) a humeral head being the main articular surface for the radius and ulna. Some small-sized amphibamiform temnospondyls have a similar humeral morphology, but they seem to have an ulnar epicondyle more developed medially (i.e., in ventral view, the ulnar epicondyle is wider than the humeral head) compared to MB.Am. 1551–1553 (Sigurdsen and Bolt 2009). As such, we consider MB.Am, 1551–1553 exhibit a humeral morphology that can only be recovered within Lissamphibia, and thus represent lissamphibian taxa, MB.Am.1554 is a fused radioulna/tibiofibula, a feature unique to Salientia (see below). Finally, MB.Am. 1555 is a poorly preserved phalanx, that does exhibit a similar morphology and size to lissamphibian ones. In the absence of non-lissamphibian specimens, we tentatively also assign MB.Am. 1555 to Lissamphibia.

MB. Am. 1551 and MB.Am. 1552 differ in the position of the humeral head relative to the diaphyseal axis and the development of the ulnar epicondyle (in MB.Am. 1552, the epicondyle is more prominent than in MB.Am.

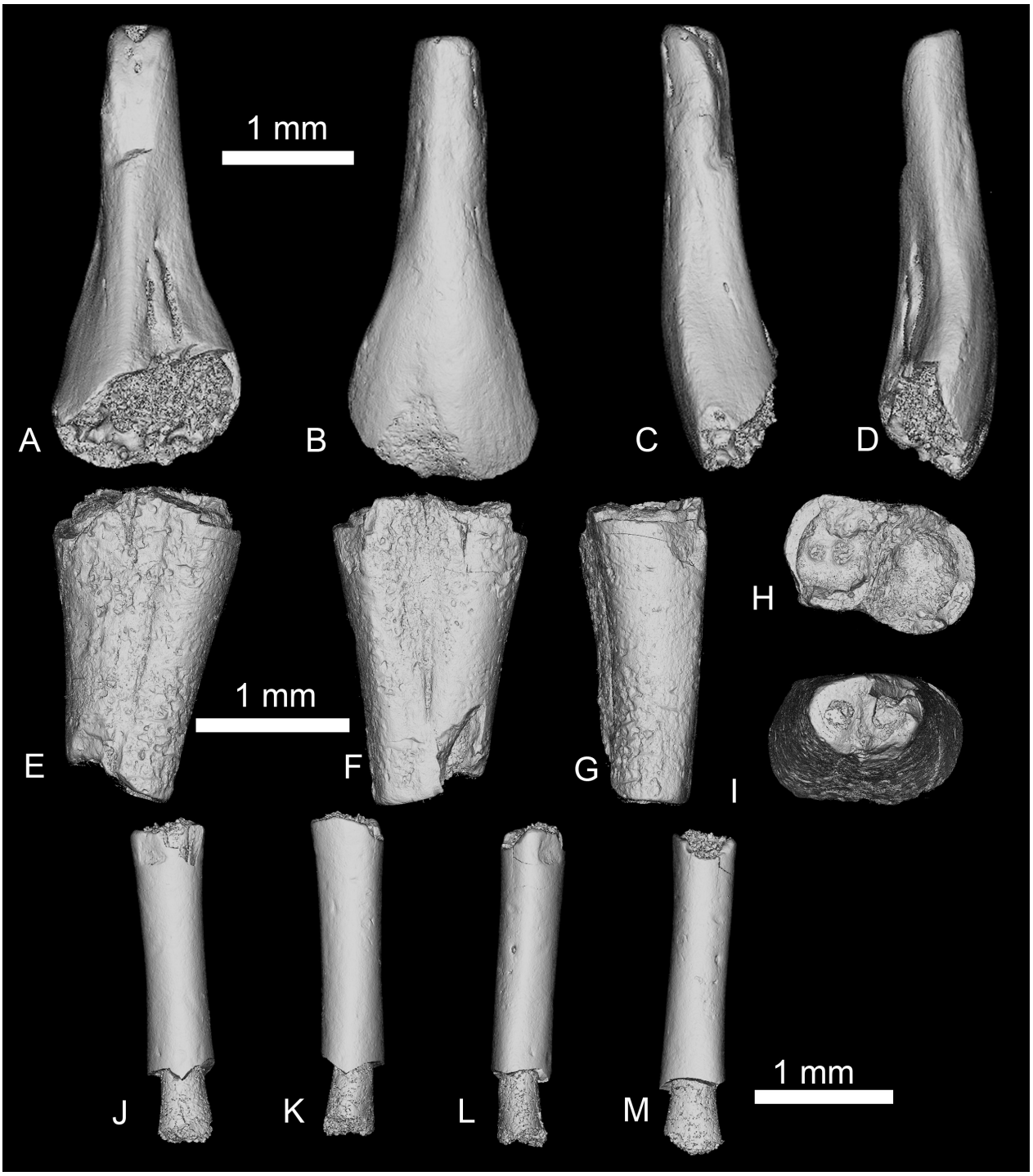

Figure 4. Indeterminate salientians of the Tendaguru Formation. **A–D.** MB. Am 1553, Salientia indet., incomplete right humerus in **A.** Ventral; **B.** Dorsal; **C.** Medial and **D.** Lateral views; **E–I.** MB. Am 1554, Salientia indet., portion of radioulna/tibiofibular in **E–F.** Dorsal/ ventral; **G.** Transversal, and **H–I.** Proximal/distal views; **J–M**, MB. Am 1555, Salientia indet., phalanx in **J–K.** Dorsal/ ventral and **L–M.** Transversal views.

1551), suggesting they represent two distinct taxa. MB. Am. 1553 does not markedly differ from either humerus but is too poorly preserved to warrant an assignment to a specific taxon. MB.Am. 1554 and 1555 cannot be assigned to a specific taxon because of their fragmentary nature. Thus, we think it is reasonable to assume that there are at least two amphibian taxa represented in the Tendaguru Formation.

Identity of amphibians in the Tendaguru Formation

In total, four clades of lissamphibians are recognized in the fossil record: Allocaudata (Albanerpetonidae), Caudata (includes Urodela), Gymnophionomorpha (includes Gymnophiona), and Salientia (includes Anura). Althrought MB. Am. 1554 is fragmentary, the presence of

a fused radioulna or tibiofibula is recovered only within Salientia (Sigurdsen and Bolt 2009; other references). It is absent within Triassic salientians, but present in some Jurassic salientians (e.g., *Notobatrachus*; Báez and Nicoli 2004, 2008) and all anurans (Sigurdsen and Bolt 2009; Keeffe and Blackburn 2020). Thus, MB. Am. 1554 is assigned to an indeterminate salientian. MB. Am. 1555 is a poorly preserved phalanx with no recognisable features and is tentatively assigned to an indeterminate salientian because no other lissamphibian clade is identified within the Tendaguru Formation (see below).

Allocaudata are represented solely by the family Albanerpetontidae (Gardner 2000). MB. Am. 1551–1553 can be excluded from this family based on a number of features (Table 2; Estes and Hoffstetter 1976; Blain et al. 2010: fig. 2L; Sweetman and Gardner 2013), the main one being the absence of a foramen on the proximal margin of the cubital fossa.

MB. Am. 1551–1553 can be excluded from all early caudate families because they exhibit a fully ossified distal region of the humeri (e.g., Evans et al. 1988, 2005; Evans and Milner 1996; Gao and Shubin 2003, 2012; Wang 2004; Wang and Rose 2005; Wang and Evans 2006a, 2006b; Averianov et al. 2008; Zhang et al. 2009; Carroll and Zheng 2012; Jia and Gao 2016a, 2016b, 2019; Jia et al. 2021; Rong et al. 2021; Jones et al. 2022; Georgalis et al. 2024). They can also be excluded from almost all extant urodele families on account of this feature (Fig. 5, Suppl. material 1: figs S1, S2). In taxa where the distal region is fully ossified (Fig. 5, Table 2; Sigurdsen and Bolt 2009: fig. 2A), MB. Am. 1551, 1552 differ in having a large humeral head width, and all three Tendaguru humeri differ from urodeles by having a reduced radial epicondyle that is indistinct in ventral view (Table 2). Within Gymnophionomorpha, only the Jurassic *Eocaecilia macropodia* Jenkins & Walsh, 1993 is known to have forelimbs. All three humeri from the Tendaguru Formation differ from *Eocaecilia* in having a reduced radial epicondyle (ectepicondyle of Jenkins et al. 2007) and MB. Am. 1551, 1552 further differ by the greater width of the humeral head and features of the cubital fossa (Table 2).

Humeri assigned to Salientia (and its crown-clade Anura) exhibit a laterally curved ventral crest (instead of medially curved within Caudata and *Eocaecilia*; see Sigurdsen et al. 2012) that differ from other lissamphibians (Suppl. material 1: figs S1, S2; Sigurdsen and Bolt 2009; Sigurdsen et al. 2012) and also lacking a dorsal

Table 2. Comparison of characters borne on the distal humeral region of Tendaguru specimens and lissamphibian clades.

Taxon/ Character	Humeral head ossification	Humeral head width ratio	Humeral head position relative to diaphyseal axis	Epicondyles development	Radial epicondyle	Ulnar epicondyle
MB. Am 1551	well-ossified	72	slightly shifted laterally from the diaphyseal axis	Asymmetrical	very reduced; indistinct in ventral view	terminates well before the level of the ventral margin of the humeral head
MB. Am 1552	well-ossified	85	in line with the diaphyseal axis	Asymmetrical	very reduced; indistinct in ventral view	terminates well before the level of the ventral margin of the humeral head
MB. Am 1553	?	?	?	?Asymmetrical	very reduced; ?indistinct in ventral view	?
Albanerpetontidae (Allocaudata)	well-ossified	<60	in line with the diaphyseal axis	Asymmetrical	reduced as a rounded projection in ventral view	terminates at the level of the ventral margin of the humeral head
Urodela (Caudata)	poorly to well ossified	40–47	shifted laterally from the diaphyseal axis	Asymmetrical	reduced as a rounded projection in ventral view	Projects mediodistally; terminates at the level of the ventral margin of the humeral head
***Eocaecilia macropodia* (Gymnomorpha)**	well-ossified	49	shifted laterally from the diaphyseal axis	Asymmetrical	reduced as a rounded projection in ventral view	terminates at the level of the ventral margin of the humeral head
***Czatkobatrachus polonicus* (Salientia)**	well ossified	65–69	shifted laterally from the diaphyseal axis	Asymmetrical	very reduced; indistinct in ventral view	terminates slightly before or at the level of the ventral margin of the humeral head

Table 2. Continued.

Taxon/ Character	Ulnar trochela (in ventral view)	Cubital fossa margins	Cubital fossa depth	Cubital fossa shape	Foramen within the cubital fossa	Olecranon scar shape
MB. Am 1551	Undistinct	poorly delimited	shallow	crescent-shape, abutting the humeral head	absent	transversally short; triangular shaped
MB. Am 1552	poorly marked, transversally very short	poorly delimited	shallow	crescent-shape, abutting the humeral head	absent	transversally short; triangular shaped
MB. Am 1553	?	?	?	?	absent	transversally short; triangular shaped
Albanerpetontidae (Allocaudata)	marked but transversally short	well delimited	deep	triangular, extending proximally on the diaphysis	present	transversally wide, hemiciruclar shape
Urodela (Caudata)	marked and transversally wide	well-delimited	shallow	cresecent shape	absent	transversally wide, hemiciruclar shape
***Eocaecilia macropodia* (Gymnomorpha)**	marked and transversally wide	well-delimited	deep	crescent shape, extending proximally on the diaphysis	absent	transversally wide, hemiciruclar shape
***Czatkobatrachus polonicus* (Salientia)**	poorly marked and transversally very short	well-delimited	shallow	triangular, extending proximally on the diaphysis	absent	transversally short; triangular shaped

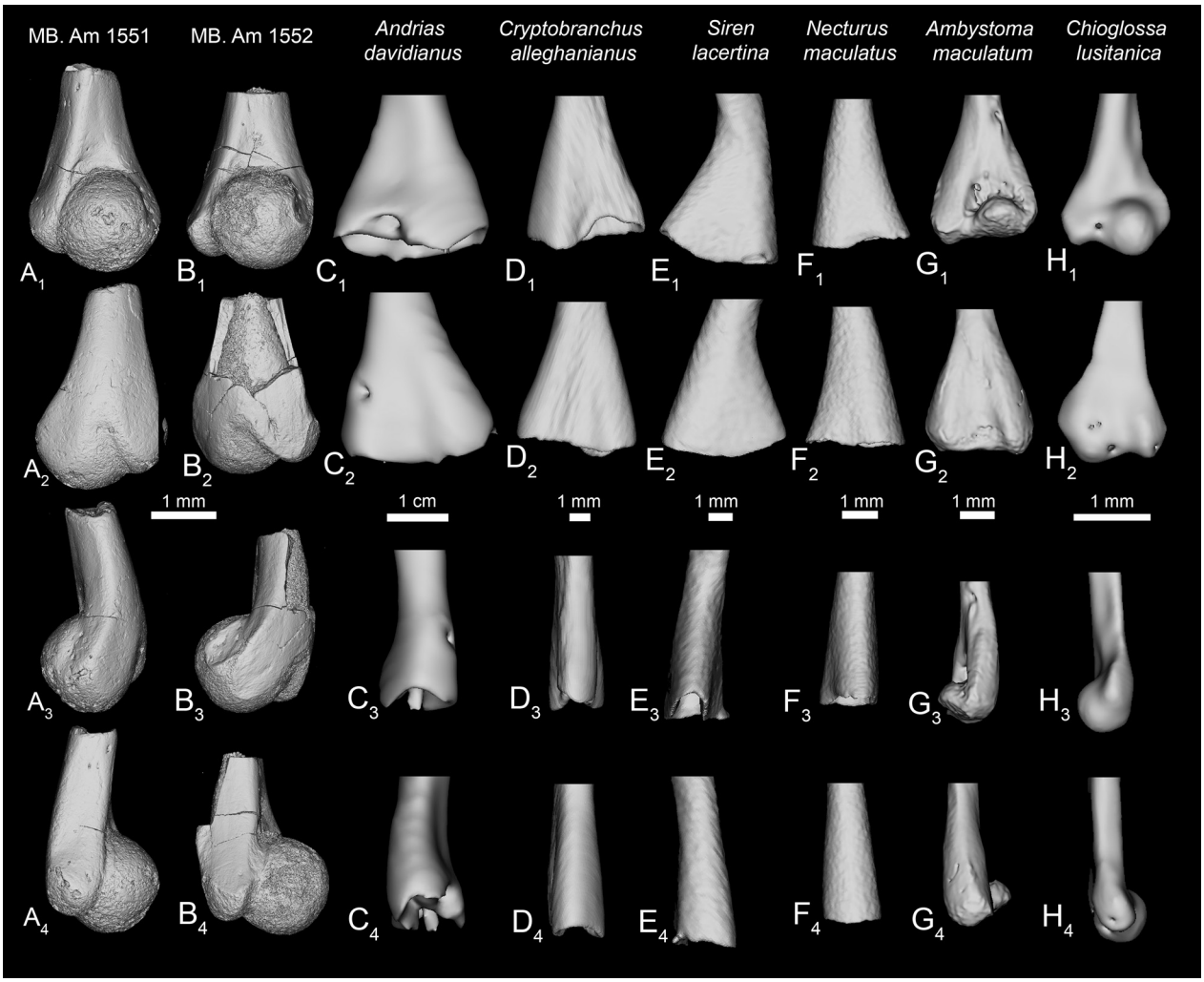

Figure 5. Humeri of Anura indet. from the Jurassic of the Tendaguru Formation and representatives of extant taxa of urodeles families. **$A_{1–4}$.** MB. Am 1551, in **A_1.** Ventral; **A_1.** Dorsal; **A_1.** Lateral and **A_1.** Medial views; **$B_{1–4}$.** MB. Am 1552, in **B_1.** Ventral; **B_2.** Dorsal; **B_3.** Lateral and **B_4.** Medial views; **$C_{1–4}$.** *Andrias davidianus* (NHMW:1/2009; Cryptobranchidae) in **C_1.** Ventral; **C_2.** Dorsal; **C_3.** Lateral and **C_4.** Medial views; **$D_{1–4}$.** *Cryptobranchus alleghanianus* (NHMUK:ZOO:1860.12.18.1-2; Cryptobranchidae) **D_1.** Ventral; **D_2.** Dorsal; **D_3.** Lateral and **D_4.** Medial views; **$E_{1–4}$.** *Siren lacertina* (UMZC:Vertebrates:R.763; Sirenidae) **E_1.** Ventral; **E_2.** Dorsal; **E_3.** Lateral and **E_4.** Medial views; **$F_{1–4}$.** *Necturus maculatus* (UMZC:Vertebrates:R.16130; Proteidae) **F_1.** Ventral; **F_2.** Dorsal; **F_3.** Lateral and **F_4.** Medial views; $G_{1–4}$. *Ambystoma maculatum* (UF:Herp:26607; Ambystomatidae) **G_1.** Ventral; **G_2.** Dorsal; **G_3.** Lateral and **G_4.** Medial views; **$H_{1–4}$.** *Chioglossa lusitanica* (MVZ:Herp:71635; Salamandridae) **H_1.** Ventral; **H_2.** Dorsal; **H_3.** Lateral and **H_4.** Medial views.

process (present in *Eocaecilia* and some urodeles; Suppl. material 1: fig. S2; Jenkins et al. 2007). Unfortunately, those features are not preserved in MB. Am. 1551–1553. However, within our sample of extinct and extant salientian (Table 3, Suppl. material 1: figs S3–S8; tables S2, S4–S5), we can highlight the following combination of features that appear unique to Salientia: (1) absence of foramen in the proximal region of the cubital fossa (shared with all lissamphibians except Allocaudata); (2) humeral head width ≥ 60 of distal humeral width (expect in Pipidae; Table 4); (3) radial epicondyle reduced to a rounded ridge that tends to be indistinct in ventral view (variable among Salientia, but a radial epicondyle that is indistinct in ventral view is unique to Salientia); (4) a transversally short olecranon scar; and (5) a transversally short ulnar trochlea. MB. Am. 1551, 1552 both exhibit this combination of characters, and half of these can be confirmed in MB. Am. 1553. As such, we assign MB. Am. 1551–1553 to Salientia, confirming the preliminary identification from Aberhan et al. (2002).

Salientia and nearly all stem-anurans lack a fully ossified distal region of the humerus (similar condition in the putative anuran *Prosalirus bitis* Shubin & Jenkins, 1995). However, studies of the preserved cartilaginous elbow joint (distal region of the humerus + ulna) of several salientians exhibit a morphology similar to *Czatkobatrachus polonicus* Evans & Borsuk-Białynicka, 1998 (Sigurdsen and Bolt 2009; Sigurdsen et al. 2012), which we consider to represent a "standard" salientian humeral morphology (Table 3). This does not markedly differ from the morphology recovered in several crown-anuran taxa (Suppl. material 1: figs S3–S4). There are two features

Table 3. Comparison of t characters borne on the distal humeral region of Tendaguru specimens, *Czatkobatrachus* (Salientia) and crown-anuran taxa from the Jurassic.

Taxon/ Character	Humeral head width ratio	Humeral head position relative to diaphyseal axis	Radial epicondyle	Ulnar epicondyle	Ulnar trochela (in ventral view)	Cubital fossa margins	Cubital fossa depth	Cubital fossa shape	Olecranon scar shape
MB. Am 1551	72	slightly shifted laterally from the diaphyseal axis	very reduced; indistinct in ventral view	terminates well before the level of the ventral margin of the humeral head	indistinct	poorly delimited	shallow	crescent-shape, abutting the humeral head	triangular shaped
MB. Am 1552	85	in line with the diaphyseal axis	very reduced; indistinct in ventral view	terminates well before the level of the ventral margin of the humeral head	poorly marked	poorly delimited	shallow	crescent-shape, abutting the humeral head	triangular shaped
MB. Am 1553	?	?	very reduced; ?indistinct in ventral view	?	?	?	?	?	triangular shaped
***Czatkobatrachus polonicus* (*Salientia*)**	65–69	slightly shifted laterally from the diaphyseal axis	very reduced; indistinct in ventral view	terminates slightly before or at the level of the ventral margin of the humeral head	poorly marked	well-delimited	shallow	triangular shaped	triangular shaped
Unknown anurans, Morrison Formation	76	slightly shifted laterally from the diaphyseal axis	very reduced; indistinct in ventral view	terminates well before the level of the ventral margin of the humeral head		poorly delimited	deep	triangular shaped	triangular shaped
***Eodiscoglossus oxoniensis* (*Anura*, *Salientia*)**	?	-	-	-	-	well-delimited	deep	-	-
Unknown anurans; Anoual	69	in line with the diaphyseal axis	very reduced; rounded in ventral view	terminates at the level of the ventral margin of the humeral head	marked	well-delimited	deep	cresecent-shaped	hemispheral shaped

that are only present within Anura: (1) a humeral head width > 70% of distal humeral width (Suppl. material 1: table S6), and (2) a reduced and crescent-shaped cubital fossa abutting the humeral head. These features are not present in all anurans (Suppl. material 1: figs S3–S8) but to our knowledge they also do not appear outside of this clade. As such, their presence in MB. Am. 1551, 1552, combined with the completely ossified distal humeral region, support an assignment to Anura. MB. Am. 1553 does not preserve its cubital fossa or its humeral head, so it cannot be allocated more specifically than Salientia.

Jurassic anuran remains that preserve the distal humerus are scarce (Evans et al. 1990; Evans and Milner 1993; Shubin and Jenkins 1995). MB. Am. 1551, 1552 both differ from known Jurassic anurans by having a shallow cubital fossa (Table 3). This suggests anurans from the Tendaguru Formation are distinct taxa from ones previously identified within other Jurassic outcrops. We compared MB. Am. 1551, 1552 to representatives of major anuran clades to determine whether referring these to specific families or clades might be possible.

Leiopelmatoidea (Ascaphidae + Leioplematidae): MB. Am. 1551, 1552 can be excluded from this earliest diverging anuran clade (Frost et al. 2006; Portik et al. 2023) by the following combination of features (Table 4, Fig. 6C, Suppl. material 1: fig. S3): (1) radial epicondyle reduced and indistinct in ventral view; (2) humeral head width > 70% distal humerus width; (3) ulnar epicondyle terminating before the ventral margin of the humeral head; and (4) a poorly developed and shallow crescentic cubital fossa.

Discoglossoidea (Bombinatoridae + Alytidae): MB-Am. 1551, 1552 differ from Bombinatoridae in having a reduced radial epicondyle that is indistinct in ventral view (Table 4, Suppl. material 1: fig. S3). MB. Am. 1551, 1552 resemble the humeral morphology of Alytidae (Table 4, Fig. 6D, Suppl. material 1: fig. S3) except for the shape of the olecranon scar; MB. Am. 1552 further differs in having its humeral head along the diaphyseal axis (Table 4, Fig. 6D, Suppl. material 1: fig. S3). In addition, both males and females of Alytidae exhibit both lateral and medial crests on the humerus, which are absent in MB. 1551, 1552 (Suppl. material 1: fig. S3).

Pipoidea (Rhinophrynidae + Pipidae): MB. Am. 1551, 1552 differ from rhinophrynids in having a slender diaphysis (the thickened diaphysis of Rhinophrynidae is likely related to fossoriality; Blackburn et al. 2019) and a triangular olecranon scar (Table 4). Both Tendaguru humeri are easily excluded from Pipidae (and its stem-clade, Pipimorpha; Gómez 2016; Lemierre et al. 2025a) because they lack the features diagnostic for this family (Table 4): (1) symmetrically developed epicondyles; (2) a deep and rounded cubital fossa; and (3) humeral head width < 60% of the distal humerus width.

Pelobatoidea: MB. Am. 1551, 1552 are closest in morphology to Pelodytidae in having a reduced radial epicondyle (Table 4, Fig. 5E, F, Suppl. material 1: fig. S4). However, they do differ from Pelodytidae in having (1) an even more reduced radial epicondyle and (2) an ulnar epicondyle that terminates well before the ventral margin of the humeral head (Fig. 6E, F, Suppl. material 1: fig. S4).

Table 4. Comparison of characters borne on the distal humeral region of Tendaguru specimens and non-neobatrachian anuran clades.

Taxon\ Character	Humeral head width ratio	Humeral head position relative to diaphyseal axis	Epicondyles development	Radial epicondyle (in ventral view)	Ulnar epicondyle	Ulnar trochela (in ventral view)	Cubital fossa margins	Cubital fossa depth	Cubital fossa shape	Olecranon scar shape
MB. Am 1551	72	slightly shifted laterally from the diaphyseal axis	Asymmetrical	very reduced; indistinct	terminates well before the level of the ventral margin of the humeral head	Indistinct	poorly delimited	shallow	crescent-shape, abutting the humeral head	triangular shaped
MB. Am 1552	85	in line with the diaphyseal axis	Asymmetrical	very reduced; indistinct	terminates well before the level of the ventral margin of the humeral head	poorly marked	poorly delimited	shallow	crescent-shape, abutting the humeral head	triangular shaped
Ascaphidae (Leiopelmatoidea)	60	slightly shifted laterally from the diaphyseal axis	Asymmetrical	reduced, protruding	terminates at the level of the ventral margin of the humeral head	well marked	well-delimited	deep	triangular, expanded proximally on the diaphysis	triangular shaped
Bombinatoridae (Discoglossoidea)	73.5	slightly shifted laterally from the diaphyseal axis	Asymmetrical	reduced, protruding	terminates well before the level of the ventral margin of the humeral head	Indistinct	poorly delimited	shallow	crescent-shape, abutting the humeral head	triangular shaped
Alytidae (Discoglossoidea)	71.5	slightly shifted laterally from the diaphyseal axis	Asymmetrical	reduced, slightly protruding	terminates well before the level of the ventral margin of the humeral head	indistinct to poorly marked	poorly delimited	shallow	crescent-shape, abutting the humeral head	hemisherical shaped
Rhinophrynidae	76.5	in line with the diaphyseal axis	Asymmetrical	reduced, indistinct	terminates well before the level of the ventral margin of the humeral head	Indistinct	well-delimited	shallow	crescent-shape, abutting the humeral head	hemisherical shaped
Pipidae	52	in line with the diaphyseal axis	Symmetrical	reduced, protruding	terminates at the level of the ventral margin of the humeral head	Indistinct	well-delimited to poorly delimited	deep	triangular, expanded proximally on the diaphysis	hemisherical shaped
Pelodytidae (Pelobatoidea)	79	slightly shifted laterally from the diaphyseal axis	Asymmetrical	reduced, slightly protruding	terminates slightly before the level of the ventral margin of the humeral head	almost indistinct	poorly delimited	shallow	crescent-shape, abutting the humeral head	triangular shaped
Pelobatidae (Pelobatoidea)	65	slightly shifted laterally from the diaphyseal axis	Asymmetrical	reduced, protruding	terminates at the level of the ventral margin of the humeral head	well marked	poorly delimited	shallow	crescent-shape, abutting the humeral head	triangular shaped
Scaphiopodidae (Pelobatoidea)	73	slightly shifted laterally from the diaphyseal axis	Asymmetrical	reduced, protruding	terminates well before the level of the ventral margin of the humeral head	poorly marked to indistinct	poorly delimited	shallow	crescent-shape, abutting the humeral head	triangular shaped
Megophryidae (Pelobatoidea)	68	slightly shifted laterally from the diaphyseal axis	Asymmetrical	reduced, protruding	terminates at the level of the ventral margin of the humeral head	poorly marked	poorly delimited	shallow	crescent-shape, abutting the humeral head	triangular shaped

Neobatrachia: There is a wide range of variation within the shape of the distal region of the neobatrachian humerus (Fig. 7, Suppl. material 1: figs S5–S18), and no specific neobatrachian traits have been identified. MB. Am. 1551, 1552 differ from the earliest diverging family Heleophrynidae (sister to all other neobatrachians; e.g., Frost et al. 2006; Jetz and Pyron 2018; Portik et al. 2023) by having (1) a poorly delimited crescentic cubital fossa and (2) an ulnar trochlea poorly marked or indistinct (Fig. 7C, Suppl. material 1: ig. S5). The humeral morphology of Heleophrynidae differs from that of other neobatrachians (Suppl. material 1: figs S5–S18) in having a rounded cubital fossa and an olecranon scar less expanded, with a rounded proximal margin. No specific humeral traits are known for the four other large neobatrachian clades: (1) Australobatrachia, (2) Hyloidea, (3) Ranoidea, and (4) Sooglossoidea.

Australobatrachia: MB. Am. 1551, 1552 differ from the morphology of Calyptocephallelidae and Myobatrachidae (the two families of Australobatrachia; Portik et al. 2023; Table 5, Fig. 7D, Suppl. material 1: fig. S5) in (1) having an indistinct radial epicondyle in ventral view and (2) having an ulnar epicondyle terminating slightly before or to the level of the ventral margin of the humeral head (Table 5, Suppl. material 1: table S5).

Hyloidea: MB. Am. 1551, 1552 differ from most hyloid families in (1) lacking a humeral head shifted laterally from the diaphyseal axis (slight shifted in MB. Am. 1552); (2) a reduced radial epicondyle that is indistinct from the humeral head in ventral view; (3) an ulnar epicondyle terminating well before the distal margin of the humeral head; and (4) an indistinct ulnar trochlea (Table 5, Fig. 7E, Suppl. material 1: figs S5–S10). Among the different hyloid families, MB. Am. 1552 most resembles the morphology of Batrachylidae, Neblinophrynidae, and Odontophrynidae (Table 5, Suppl. material 1: figs S5–S10).

Ranoidea: MB. Am. 1551, 1552 lack the robust humeral morphology of families with obligate fossorial species (e.g., Brevicipitidae, Hemisotidae; Table 5). MB. Am. 1552 resembles many ranoid taxa in the following traits (Table 5, Fig. 7F, Suppl. material 1: figs S11–S18): (1) humeral head aligned with the diaphyseal axis; (2) radial epicondyle indistinct in ventral view; and

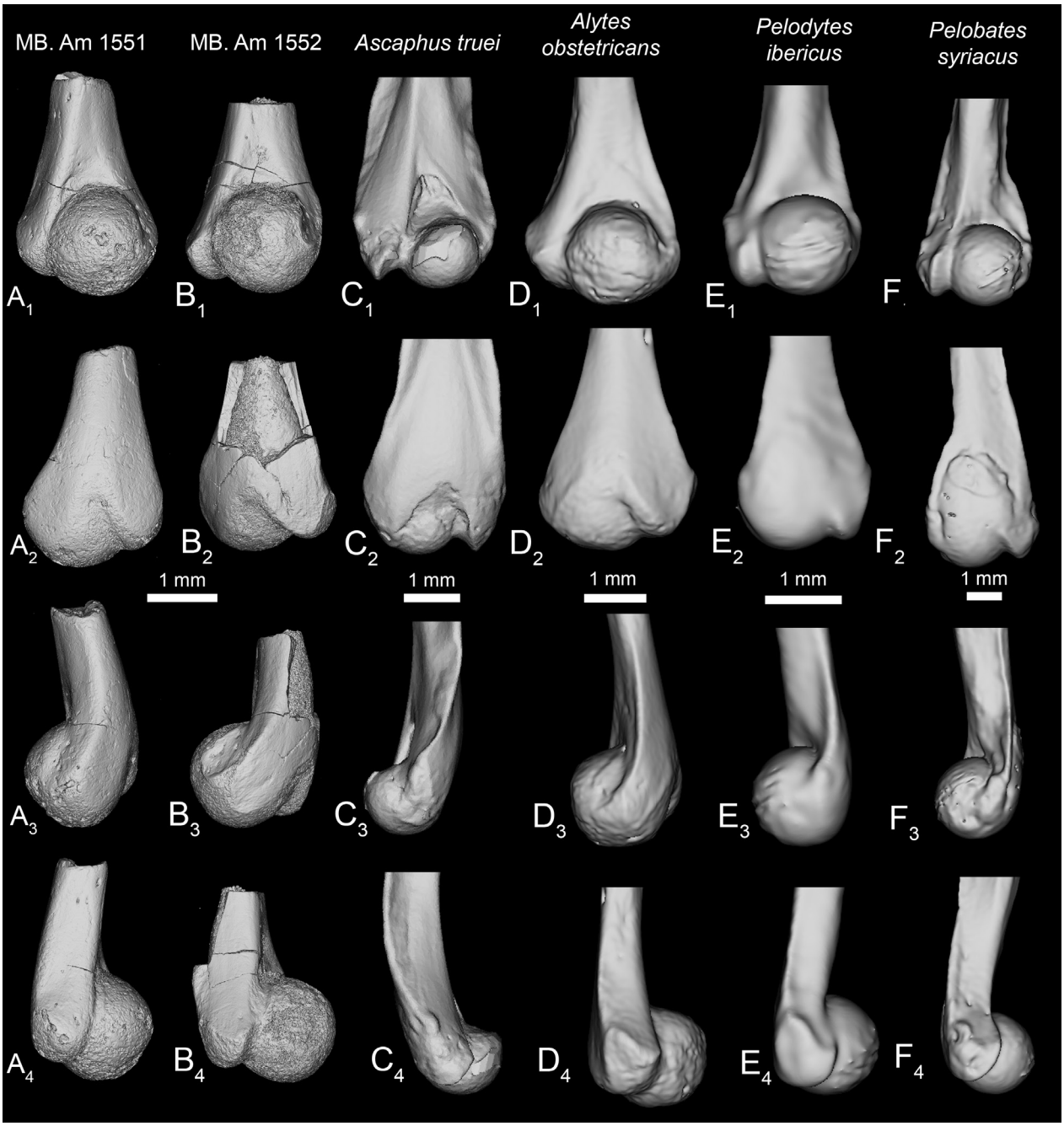

Figure 6. Humeri of Anura indet. from the Jurassic of the Tendaguru Formation and representatives of non-neobatrachian anuran clades **$A_{1–4}$.** MB. Am 1551, in **A_1.** Ventral; **A_1.** Dorsal; **A_1.** Lateral and **A_1.** Medial views; **$B_{1–4}$.** MB. Am 1552. In **B_1.** Ventral; **B_2.** Dorsal; **B_3.** Lateral and **B_4.** Medial views; **$C_{1–4}$.** *Ascaphus truei* (UF:Herp:80664; Leipelmatoidea) in **C_1.** Ventral; **C_2.** Dorsal; **C_3.** Lateral and **C_4.** Medial views; **$D_{1–4}$.** *Alytes obstetricans* (YPM:VZs:004877; Discoglossoidea) **D_1.** Ventral; **D_2.** Dorsal; **D_3.** Lateral and **D_4.** Medial views; **$E_{1–4}$.** *Pelodytes ibericus* (MVZ:Herp:186009; Pelodytidae) **E_1.** Ventral; **E_2.** Dorsal; **E_3.** Lateral and **E_4.** Medial views; **$F_{1–4}$.** *Pelobates syriacus* (MVZ:Herp:234651; Pelobatidae) **F_1.** Ventral; **F_2.** Dorsal; **F_3.** Lateral and **F_4.** Medial views.

(3) poorly delimited crescentic cubital fossa abutting the humeral head. MB. Am. 1552 differs from most ranoids (except Mantellidae) in having a poorly delimited ulnar trochlea (Table 5).

Sooglossoidea: Both MB. Am. 1551, 1552 differ from the robust humeral morphology (Table 5, Fig. 7G, Suppl. material 1: fig. S18) of the fossorial *Nasikabatrachus* (sole genus of Nasikabatrachidae). They differ from Sooglossidae in lacking a protruding radial epicondyle and a marked ulnar trochlea (Table 5, Fig. 7G).

The phylogenetic relationships of MB. Am. 1551, 1552 within Anura are difficult to resolve. They can be excluded from several clades, especially those with traits linked to obligate aquatic or fossorial lifestyles. The combination in MB. Am. 1551, 1552 of a (1) humeral head width > 70% distal humerus width, (2) radial epicondyle indistinct in ventral view, (3) poorly delimited and crescentic cubital fossa, and (4) triangular olecranon scar are reminiscent of several neobatrachian families (Table 5, Suppl. material 1: figs

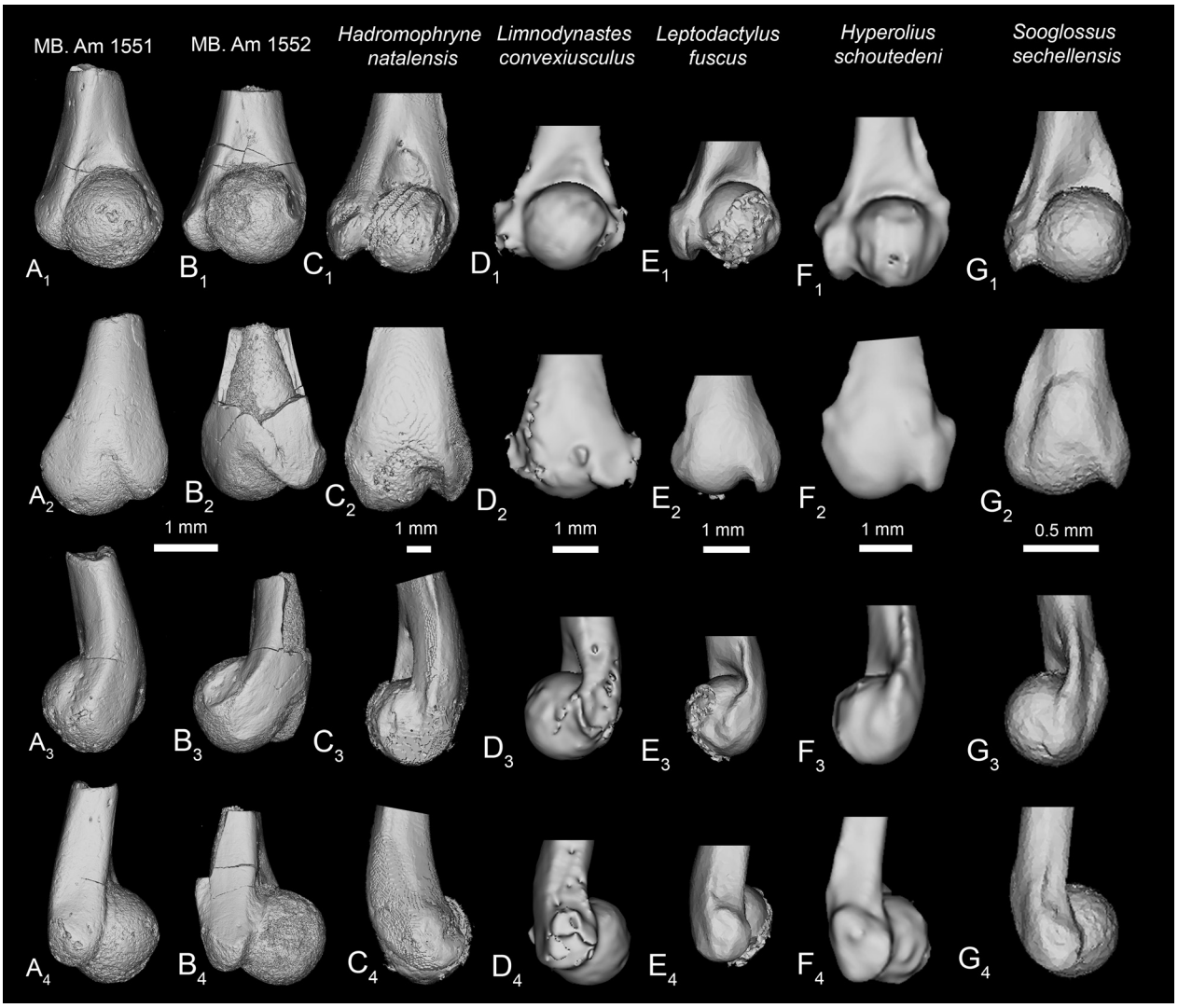

Figure 7. Humeri of Anura indet. from the Jurassic of the Tendaguru Formation and representatives of neobatrachian taxa. **$A_{1–4}$.** MB. Am 1551, in **A_1.** Ventral; **A_1.** Dorsal; **A_1.** Lateral and **A_1.** Medial views; **$B_{1–4}$.** MB. Am 1552. In **B_1.** Ventral; **B_2.** Dorsal; **B_3.** Lateral and **B_4.** Medial views; **$C_{1–4}$.** *Hadromophryne natalensis* (UF:Herp:100828; Heleophrynidae) in **C_1.** Ventral; **C_2.** Dorsal; **C_3.** Lateral and **C_4.** Medial views; **$D_{1–4}$.** *Limnodynastes convexiusculus* (CAS:HERP:121263; Myobatrachidae, Australobatrachia) **D_1.** Ventral; **D_2.** Dorsal; **D_3.** Lateral and **D_4.** Medial views; **$E_{1–4}$.** *Leptodactylus fuscus* (UF:Herp:103637; Leptodactylidae, Hyloidea) **E_1.** Ventral; **E_2.** Dorsal; **E_3.** Lateral and **E_4.** Medial views; **$F_{1–4}$.** *Hyperolius schoutedeni* (UF:Herp:185889; Afrobatrachia, Ranoidea) **F_1.** Ventral; **F_2.** Dorsal; **F_3.** Lateral and **F_4.** Medial views; **$G_{1–4}$.** *Sooglossus sechellensis* (CAS:HERP:160084; Sooglossidae) **G_1.** Ventral; **G_2.** Dorsal; **G_3.** Lateral and **G_4.** Medial views.

S5–S18). It is tempting to refer these two humeri to the Neobatrachia, but the morphology is also reminiscent of the Alytidae (Discoglossoidea) and Pelodytidae (Pelobatoidea). As such, we conservatively assign MB. Am. 1551, 1552 to indeterminate Anura.

Lissamphibians from the Jurassic of continental Africa

Although Lissamphibia likely had a global distribution by the end of the Triassic, this clade is absent from the fossil record of continental Africa and South America until the early/ middle Jurassic (Jones et al. 2003; Gardner and Rage 2016; Haddoumi et al. 2016). Jurassic lissamphibian occurrences are restricted to northern continental Africa, which has been considered closer to affinity to Laurasian faunas (Eurasia + North America) than Gondwanan (South America, Africa, Antarctica, India, Madagascar, Australia) (Lasseron et al. 2020). Within the northern African faunas, albanerpetontids and salamanders are known (Gardner and Rage 2016) whereas anurans have only been identified within the Upper Jurassic-Lower Cretaceous locality of Anoual (Lasseron et al. 2020). As such, the anurans taxa identified here from the Tendaguru Formation represent the oldest occurrence of lissamphibians within sub-Saharan Africa and oldest anuran occurrence within continental Africa. Because both *Notobatrachus* and *Vieraella* from South America are recognized as outside the crown-group Anura, these Tendaguru specimens also represent the oldest occurrence of Anura within Gondwana.

Table 5. Comparison of characters borne on the distal humeral region of Tendaguru specimens and neobatrachian families.

Taxon/Character	Humeral head width ratio	Humeral head position relative to diaphyseal axis	Radial epicondyle (ventral view)	Ulnar epicondyle	Ulnar trochela (in ventral view)	Cubital fossa margins	Cubital fossa depth	Olecranon scar shape
MB. Am 1551	72.0	slightly shifted laterally from the diaphyseal axis	indistinct	terminates well before the level of the ventral margin of the humeral head	indistinct	poorly	shallow	triangular shaped
MB. Am 1552	85	in line with the diaphyseal axis	indistinct	terminates well before the level of the ventral margin of the humeral head	poorly marked	poorly	shallow	triangular shaped
Heleophrynidae	64	slightly shifted laterally from the diaphyseal axis	protruding	terminates slightly before or to the level of the ventral margin of the humeral head	well-marked	well-	moderatly deep	rounded proximally
Calyptocephalellidae (Australobatrachia)	68	shifted laterally from the diaphyseal axis	protruding	terminates slightly before or to the level of the ventral margin of the humeral head	poorly marked	poorly	shallow	triangular shaped
Myobatrachidae (Australobatrachia)	65	slightly shifted laterally from the diaphyseal axis	protruding	terminates slightly before or to the level of the ventral margin of the humeral head	well marked	poorly	shallow	triangular shaped
Allophrynidae (Hyloidea)	69	slightly shifted laterally from the diaphyseal axis	protruding	terminates at the level of the ventral margin of the humeral head	well marked	poorly	shallow	triangular shaped
Alsodidae (Hyloidea)	77	slightly shifted laterally from the diaphyseal axis	protruding	terminates at the level of the ventral margin of the humeral head	poorly marked	poorly	shallow	triangular shaped
Batrachylidae (Hyloidea)	79.5	in line with the diaphyseal axis	protruding	?	?	poorly	shallow	triangular shaped
Brachycephalidae (Terrana, Hyloidea)	63	shifted laterally from the diaphyseal axis	protruding	terminates at the level of the ventral margin of the humeral head	well marked	well-	shallow	triangular shaped
Bufonidae (Hyloidea)	68	shifted laterally from the diaphyseal axis	protruding to indstinct	terminates at the level of the ventral margin of the humeral head	well to poorly marked	poorly	shallow	triangular shaped
Caligrophynidae (Terrana, Hyloidea)	67	slightly shifted laterally from the diaphyseal axis	protruding	terminates at the level of the ventral margin of the humeral head	well marked	poorly	shallow	triangular shaped
Centrolenidae (Hyloidea)	64	slightly shifted laterally from the diaphyseal axis	protruding	terminates at the level of the ventral margin of the humeral head	well marked	poorly	shallow	triangular shaped
Ceratophryidae (Hyloidea)	59	slightly shifted laterally from the diaphyseal axis	protruding	terminates at the level of the ventral margin of the humeral head	poorly marked	poorly	shallow	triangular shaped
Ceuthomantidae (Terrana, Hyloidea)	75.5	mostly in line with the diaphyseal axis	protruding	?terminates at the level of the ventral margin of the humeral head	?	poorly	shallow	triangular shaped
Craugastoridae (Terrana, Hyloidea)	67	slightly shifted laterally from the diaphyseal axis	slightly protruding	terminates at the level of the ventral margin of the humeral head	well marked	poorly	shallow	triangular shaped
Cycloramphidae (Hyloidea)	67.5	slightly shifted laterally from the diaphyseal axis	protruding	terminates at the level of the ventral margin of the humeral head	well marked	poorly	shallow	triangular shaped
Dendobatidae (Hyloidea)	69	in line with the diaphyseal axis	protruding	terminates at the level of the ventral margin of the humeral head	well marked	poorly	shallow	triangular shaped
Eleutherodactylidae (Terrana, Hyloidea)	64	shifted laterally from the diaphyseal axis	protruding	terminates at the level of the ventral margin of the humeral head	well marked	poorly	shallow	triangular shaped
Hemiphractidae (Hyloidea)	66	shifted laterally from the diaphyseal axis	protruding	terminates at the level of the ventral margin of the humeral head	well marked	poorly	shallow	triangular shaped
Hylidae (Hyloidea)	62	slightly shifted laterally from the diaphyseal axis	protruding	terminates at the level of the ventral margin of the humeral head	well marked	poorly	shallow	triangular shaped
Hylodidae (Hyloidea)	61	shifted laterally from the diaphyseal axis	indistinct	terminates at the level of the ventral margin of the humeral head	well marked	poorly	shallow	triangular shaped
Leptodactylidae (Hyloidea)	65.5	shifted laterally from the diaphyseal axis	slightly protruding	terminates at the level of the ventral margin of the humeral head	well to poorly marked	well-	shallow	triangular shaped
Neblinophrynidae (Terrana, Hyloidea)	65.5	in line with the diaphyseal axis	slightly protruding	terminates slightly before the level of the ventral margin of the humeral head	well marked	poorly	shallow	triangular shaped
Odontophrynidae (Hyloidea)	66	in line with the diaphyseal axis	slightly protruding	terminates slightly before the level of the ventral margin of the humeral head	poorly marked	poorly	shallow	triangular shaped

Taxon/Character	Humeral head width ratio	Humeral head position relative to diaphyseal axis	Radial epicondyle (ventral view)	Ulnar epicondyle	Ulnar trochela (in ventral view)	Cubital fossa margins	Cubital fossa depth	Olecranon scar shape
Rhinodermatidae (Hyloidea)	73.5	shifted laterally from the diaphyseal axis	slightly protruding/ indistinct	terminates at the level of the ventral margin of the humeral head	well marked	well-	shallow	triangular shaped
Strabomantidae (Terrana, Hyloidea)	68	slightly shifted laterally from the diaphyseal axis	slightly protruding	terminates at the level of the ventral margin of the humeral head	well marked	poorly	shallow	triangular shaped
Telmatobiidae (Hyloidea)	67	shifted laterally from the diaphyseal axis	slightly protruding/ indistinct	terminates at the level of the ventral margin of the humeral head	well marked	well-	shallow	triangular shaped
Brevicipidae (Afrobatrachia, Ranoidea)	57	shifted laterally from the diaphyseal axis	protruding	terminates well before the level of the ventral margin of the humeral head	well marked	well-	shallow	triangular shaped
Hemisotidae (Afrobatrachia, Ranoidea)	55	shifted laterally from the diaphyseal axis	protruding	terminates at the level of the ventral margin of the humeral head	well marked	poorly	shallow	triangular shaped
Hyperoliidae (Afrobatrachia, Ranoidea)	65	slightly shifted laterally from the diaphyseal axis to in line with the diaphyseal axis	protruding to indistinct	terminates slightly before or to the level of the ventral margin of the humeral head	well marked to poorly marked	poorly	shallow	triangular shaped
Arthroleptidae (Afrobatrachia, Ranoidea)	67	mostly in line with the diaphyseal axis	protruding to indistinct	terminates at the level of the ventral margin of the humeral head	well marked	poorly	shallow	triangular shaped
Microhylidae (Ranoidea)	73	mostly in line with the diaphyseal axis	indistinct	terminates at the level of the ventral margin of the humeral head	well marked	poorly	shallow	triangular shaped
Ranidae (Natatanura, Ranoidea)	73	mostly in line with the diaphyseal axis	slightly protruding to indistinct	terminates at the level of the ventral margin of the humeral head	well marked	poorly	shallow	triangular shaped
Mantellidae (Natatanura, Ranoidea)	70.5	mostly in line with the diaphyseal axis	indistinct	terminates at the level of the ventral margin of the humeral head	well marked	poorly	shallow	triangular shaped
Micrixalidae (Natatanura, Ranoidea)	70	mostly in line with the diaphyseal axis	indistinct	terminates slightly before or to the level of the ventral margin of the humeral head	poorly marked	poorly	shallow	triangular shaped
Nyctibatrachidae (Natatanura, Ranoidea)	63	slightly shifted laterally from the diaphyseal axis	protruding	terminates slightly before the level of the ventral margin of the humeral head	poorly marked	poorly	shallow	triangular shaped
Ranixalidae (Natatanura, Ranoidea)	77	mostly in line with the diaphyseal axis	indistinct	terminates at the level of the ventral margin of the humeral head	well marked	poorly	shallow	triangular shaped
Ceratobrachidae (Natatanura, Ranoidea)	76	mostly in line with the diaphyseal axis	protruding	terminates at the level of the ventral margin of the humeral head	well marked	poorly	shallow	triangular shaped
Dicroglossidae (Natatanura, Ranoidea)	77	mostly in line with the diaphyseal axis	protruding	terminates slightly before the level of the ventral margin of the humeral head	?indistinct	poorly	shallow	triangular shaped
Rhacophoridae (Natatanura, Ranoidea)	67	slightly shifted laterally from the diaphyseal axis	protruding	terminates slightly before the level of the ventral margin of the humeral head	well marked	poorly	shallow	triangular shaped
Conrauidae (Natatanura, Ranoidea)	68	slightly shifted laterally from the diaphyseal axis	protruding	terminates at the level of the ventral margin of the humeral head	well marked	well-	shallow	triangular shaped
Odontobatrachidae (Natatanura, Ranoidea)	64	mostly in line with the diaphyseal axis	slightly protruding	terminates well before the level of the ventral margin of the humeral head	poorly marked	poorly	shallow	triangular shaped
Petropedetidae (Natatanura, Ranoidea)	65	slightly shifted laterally from the diaphyseal axis	slightly protruding	terminates at the level of the ventral margin of the humeral head	well marked	well-	shallow	triangular shaped
Phrynobatrachidae (Natatanura, Ranoidea)	71	slightly shifted laterally from the diaphyseal axis to in line with the diaphyseal axis	indistinct	terminates at the level of the ventral margin of the humeral head	well marked	poorly	shallow	triangular shaped
Ptychadenidae (Natatanura, Ranoidea)	71	mostly in line with the diaphyseal axis	protruding to indistinct	terminates at the level of the ventral margin of the humeral head	well marked	poorly	shallow	triangular shaped
Pyxicephalidae (Natatanura, Ranoidea)	71	slightly shifted laterally from the diaphyseal axis to in line with the diaphyseal axis	protruding to indistinct	terminates slightly before or to the level of the ventral margin of the humeral head	well marked	poorly	shallow	triangular shaped
Nasikabatrachidae (Sooglossoidea)	70	shifted laterally from the diaphyseal axis	protruding	terminates slightly before or to the level of the ventral margin of the humeral head	well-marked	poorly	shallow	triangular shaped
Sooglossidae (Sooglossoidea)	75.5	slightly shifted laterally from the diaphyseal axis	protruding	terminates slightly before or to the level of the ventral margin of the humeral head	well-marked	poorly	shallow	triangular shaped

Conclusion

The five lissamphibian specimens from the Upper Jurassic of the Tendaguru Formation (Tendaguru Hill, Tanzania) are identified as three incomplete humeri, a radioulna/tibiofibular, and a phalanx, with the two humeri likely representing two taxa. The humeri and radioulna/ tibiofibula can be referred to Salientia. Our comparisons with stem- and crown-anurans highlight a combination of characters that are shared between two Tendaguru humeri and crown-anurans: (1) a humeral head width > 70% of distal humeral width (not present in all anurans; Suppl. material 1: table S6), and (2) a reduced and crescent-shaped cubital fossa abutting the humeral head. The morphology of these humeri falls within the variation of neobatrachians but is also similar to the Alytidae and Pelodytidae, preventing an assignment of these Tendaguru specimens more specifically than Anura. These humeri represent the oldest occurrence of Anura (and thus Salientia) from continental Africa and the oldest occurrences of Anura within Jurassic outcrops of Gondwana. Our study suggests that the Tendaguru Formation and other Africa Jurassic localities may hold important discoveries on the early diversification of Gondwanan frogs.

Funding

A. Lemierre was supported by a Dr. Betsy Nicholls Postdoctoral Research Fellowship, provided by the Royal Tyrrell Museum Cooperating Society (Drumheller, AB, Canada). Funding for CT-scans of the many comparative specimens used in this study was supported largely from the US National Science Foundation (DBI-1701714 to D. Blackburn).

Acknowledgments

We thank F. Witzmann (Museum für Naturkunde Berlin) for access to the specimens, K. Mahlow-Tillack (Museum für Naturkunde Berlin) for scanning all amphibian specimens from Tendaguru kept at the Museum für Naturkunde Berlin and R. Bussert (Technische Universität Berlin) for comments on the manuscript. We thank F. Witzmann for his editorial work and comments on this manuscript. We also thank H.-A. Blain (Institut català de Paleoecologia Humana i Evolució Social), Georgios Georgalis (Institute of Systematics and Evolution of Animals, Polish Academy of Sciences), and an anonymous reviewer for their comments and edits on this manuscript.

References

Aberhan M, Bussert R, Heinrich W-D, Schrank E, Schultka S, Sames B, Kriwet J, Kapilima S (2002) Palaeoecology and depositional environments of the Tendaguru Beds (Late Jurassic to Early Cretaceous, Tanzania). Mitteilungen aus dem Museum für Naturkunde in Berlin, Geowissenschaftliche Reihe 5: 19–44. https://doi.org/10.1002/mmng.4860050103

Aitken G (1961) Geology and Palaeontology of the Jurassic and Cretaceous of Southern Tanganyika. Bulletin of the Geological Survey of Tanganyika 31: 1–144.

Arratia G, Kriwet J, Heinrich W-D (2002) Selachians and Actinopterygians from the Upper Jurassic of Tendaguru, Tanzania. Mitteilungen aus dem Museum für Naturkunde in Berlin, Geowissenschaftliche Reihe 5: 207–228. https://doi.org/10.1002/mmng.4860050112

Averianov AO, Martin T, Skutschas PP, Rezyi AS, Bakirov AA (2008) Amphibians from the Middle Jurassic Balabansai Svita in the Fergana depression, Kyrgyzstan (Central Asia). Palaeontology 51(2): 471–485. https://doi.org/10.1111/j.1475-4983.2007.00748.x

Báez AM, Basso NG (1996) The earliest known frogs of the Jurassic of South America: Review and cladistic appraisal of their relationships. Münchner Geoswiss Abhladungen 30: 131–158.

Báez AM, Nicoli L (2004) A new look at an old frog: the Jurassic *Notobatrachus* Reig from Patagonia. Ameghiniana 41: 257–270.

Báez AM, Nicoli L (2008) A new species of *Notobatrachus* (Amphibia, Salientia) from the Middle Jurassic of northwestern Patagonia. Journal of Palaeontology 82: 372–376. https://doi.org/10.1666/06-117.1

Báez AM, Nicoli L (2025) Re-examination of the oldest known frog from South America: New data prompt new evolutionary interpretations. The Anatomical Record. https://doi.org/10.1002/ar.25654

Bailon S (1999) Différenciation ostéologique des anoures (Amphibia, Anura) de France. In: Desse J, Desse-Berset N (Eds) Centre de Recherches Archéologiques du CNRS.

Barcelos LA, dos Santos RO (2023) The lissamphibian fossil record of South America. Palaeobiodiversity and Palaeoenvironments 103: 341–405. https://doi.org/10.1007/s12549-022-00536-0

Blackburn DC, Roberts L, Vallejo-Pareja MC, Stanley EL (2019) First record of the anuran family Rhinophrynidae from the Oligocene of Eastern North America. Journal of Herpetology 53(4): 316–323. https://doi.org/10.1670/19-044

Blackburn DC, Boyer DM, Gray JA, Winchester J, Bates JM, Baumgart SL, Braker E, Coldren D, Conway KW, Davis Rabosky A, de la Sancha N, Dillman CB, Dunnum JL, Early CM, Frable BW, Gage MW, Hanken J, Maisano JA, Marks BD, Maslenikov KP, McCormack JE, Nagesan RS, Pandelis GG, Prestridge HL, Rabosky DL, Randall ZS, Robbins MB, Scheinberg LA, Spencer CL, Summers AP, Tapanila L, Thompson CW, Tornabene L, Watkins-Colwell GJ, Welton LJ, the oVert Project Team, Stanley EL (2024) Increasing the impact of vertebrate scientific collections through 3D-imaging: the openVertebrate (oVert) Thematic Collections Network. BioScience 74: 169–186. https://doi.org/10.1093/biosci/biad120

Blain HA, Canudo J-I, Cuenca-Bescós G, López-Matínez N (2010) Amphibians and squamate reptiles from the latest Maastrichtian (Upper Cretaceous) of Blasi 2 (Huesca, Spain). Cretaceous Research 31(4): 433–446. https://doi.org/10.1016/j.cretres.2010.06.001

Bolkay STJ (1919) Osnove uporedne osteologije anurokih batrahija sa dodatkom o porijekly anura I sa skicom naravnoga Sistema istih [Elements of the comparative osteology of the tailless batrachians with an appendix on the probable origin of the anurous batrachians and a sketch of their natural system. Glasnik zemaljskog muzeja u Bosni i Hercegovini, Sarajevo 31: 277–357. [In Slovene]

Bussert R, Aberhan M (2004) Storms and tsunamis: evidence of event sedimentation in the late Jurassic Tendaguru Beds of southeastern Tanzania. Journal of African Earth Sciences 39: 549–555. https://doi.org/10.1016/j.jafrearsci.2004.07.008

Bussert R, Heinrich W-D, Aberhan M (2009) The Tendaguru Formation (Late Jurassic to Early Cretaceous, southern Tanzania): definition,

palaeoenvironments, and sequence stratigraphy. Fossil Record 12: 141–174. https://doi.org/10.1002/mmng.200900004

Carroll R, Zheng A (2012) A neotenic salamander, *Jeholotriton paradoxus*, from the Daohugou Beds in Inner Mongolia, Zoological Journal of the Linnean Society 164: 659–668. https://doi.org/10.1111/j.1096-3642.2011.00777.x

Chen J, Bever GS, Yi H-Y, Norell M (2016) A burrowing frog from the late Paleocene of Mongolia uncovers a deep history of spadefoot toads (Pelobatoidea) in East Asia. Scientific Reports 6(1): 19209. https://doi.org/10.1038/srep19209

Delfino M (2020) Early Pliocene anuran fossils from Kanapoi, Kenya, and the first fossil record for the African burrowing frog *Hemisus* (Neobatrachia: Hemisotidae). Journal of Human Evolution 140: 102353. https://doi.org/10.1016/j.jhevol.2017.06.008

Duellman WE, Trueb L (1986) Biology of amphibians. McGaw-Hill (New York, USA). https://doi.org/10.2307/1445022

Estes R, Hoffstetter R (1976) Les urodèles du Miocène de la Grive Saint-Alban (Isère, France). Bulletin du Muséum National d'Histoire Naturelle, 3ème série 398: 297–343.

Estes R, Reig OA (1973) The early fossil record of frogs: a review of the evidence. In: Vidal JL (Ed.) Evolutionary biology of the anurans. Contemporary research on major problems. University of Missouri Press (Columbia, USA): 11–63.

Estes R, Sanchíz B (1982) New discoglossid and palaeobatrachid frogs from the Late Cretaceous of Wyoming and Montana, and a review of other frogs form the Lance and Hell Creek Formations. Journal of Vertebrate Paleontology 2(1): 9–20. https://doi.org/10.1080/02724634.1982.10011914

Evans SE, Borsuk-Białynicka M (1998) A stem-group frog from the Early Triassic of Poland. Acta Palaeontologica Polonica 43: 573–580.

Evans SE, Borsuk-Białynicka M (2009) The Early Triassic stem-frog *Czatkobatrachus* from Poland. Palaeontologica Polonica 65: 79–105.

Evans SE, Milner AR (1993) Frogs and salamanders from the Upper Jurassic Morrison Formation (Quarry Nine, Como Bluff) of North America. Journal of Vertebrate Paleontology 13: 24–30. https://doi.org/10.1080/02724634.1993.10011485

Evans SE, Milner AR (1996) A metamorphosed salamander from the early Cretaceous of Las Hoyas, Spain. Philosophical Transactions of the Royal Society of London: Biological Sciences 351(1340): 627–646. https://doi.org/10.1098/rstb.1996.0061

Evans SE, Milner AR, Musset F (1988) The earliest known salamanders (Amphibia, Caudata): A record from the Middle Jurassic of England. Geobios 21(5): 539–552. https://doi.org/10.1016/S0016-6995(88)80069-X

Evans SE, Milner AR, Musset F (1990) A discoglossid frog from the Middle Jurassic of England. Palaeontology 33: 299–311.

Evans SE, Lally C, Chure DC, Elder A, Maisano JA (2005) A Late Jurassic salamander (Amphibia: Caudata) from the Morrison Formation of North America. Zoological Journal of the Linnean Society 143: 599–616. https://doi.org/10.1111/j.1096-3642.2005.00159.x

Frazão A, da Silva HR, de Moraes Russo CA (2015) The Gondwana breakup and the history of the Atlantic and Indian Oceans unveils two new clades for early neobatrachian diversification. PLoS ONE 10(11): e0143926. https://doi.org/10.1371/journal.pone.0143926

Fedorov A, Beichel R, Kalpathy-Cramer J, Finet J, Fillion-Robin J-C, Pujol S, Bauer C, Jennings D, Fennessy FM, Sonka M, Buatti J, Aylward SR, Miller JV, Pieper S, Kikinis R (2012) 3D Slicer as an image computing platform for the Quantitative Imaging Network. Magnetic Resonance Imaging 30(9): 1323–1341. https://doi.org/10.1016/j.mri.2012.05.001

Feng Y-J, Blackburn DC, Liang D, Hillis DM, Wake DB, Cannatella DC, Zhang P (2017) Phylogenomics reveals rapid, simultaneous diversification of three major clades of Gondwanan frogs at the Cretaceous-Paleogene boundary. Proceedings of the National Academy of Sciences 114(29): E5864–E5870. https://doi.org/10.1073/pnas.1704632114

Fouquet A, Kok PJR, Recoder RS, Prates I, Camacho A, Marques-Souza S, Ghellere JM, McDiarmid RW, Rodrigues MT (2024) Relicts in the mist: Two new frog families, genera and species highlight the role of Pantepui as a biodiversity museum throughout the Cenozoic. Molecular Phylogenetics and Evolution 191(107971): 1–22. https://doi.org/10.1016/j.ympev.2023.107971

Frost DR (2025) Amphibian species of the world: an online reference. Version 6.2 (24/02/2025). [Retrieved July 11th, 2025] https://amphibiansoftheworld.amnh.org/index.php

Frost DR, Grant T, Faivovich J, Bain RH, Haas A, Haddad CFB, De Sá RO, Channing A, Wilkinson M, Donnellan SC, Raxworthy CJ, Campbell JA, Blotto BL, Moler P, Drewes RC, Nussbaum RA, Lynch JD, Green DM, Wheeler WC (2006) The Amphibian tree of life. Bulletin of the American Museum of Natural History 297: 1–291. https://doi.org/10.1206/0003-0090(2006)297[0001:TATOL]2.0.CO;2

Gao K-Q, Shubin NH (2003) Earliest known crown-group salamanders. Nature 422: 424–428. https://doi.org/10.1038/nature01491

Gao K-Q, Shubin NH (2012) Late Jurassic salamandroid from Western Liaoning, China. Proceedings of the National Academy of Sciences of the United States of America 109: 5767–5772. https://doi.org/10.1073/pnas.1009828109

Gardner JD (2000) Revised taxonomy of albanerpetontid amphibians. Acta Palaeontologica Polonica 45(1): 55–70.

Gardner JD, Rage J-C (2016) The fossil record of lissamphibians from Africa, Madagascar, and the Arabian Plate. Palaeobiodiversity and Palaeoenvironments 96(1): 169–220. https://doi.org/10.1007/s12549-015-0221-0

Gaupp E (1896) Ecker's und Wiedersheim's Anatomie des Frosches, Vol. I, Lehre vom skelet und vom muskelsystem. 3rd edn., Braunschweig, Germany: Verlag von Friedrich Vieweg und Sohn, 264 pp.

Georgalis GL, Villa A, Ivanov M, Delfino M (2024) New diverse amphibian and reptile assemblages from the late Neogene of northern Greece provide novel insights into the emergence of extant herpetofaunas of the southern Balkans. Swiss Journal of Palaeontology 143: 34 [91 pp.]. https://doi.org/10.1186/s13358-024-00332-7

Gómez RO (2016) A new pipid frog from the Upper Cretaceous of Patagonia and early evolution of crown-group Pipidae. Cretaceous Research 62: 52–64. https://doi.org/10.1016/j.cretres.2016.02.006

Gómez RO, Turazzini GF (2021) The fossil record and phylogeny of South American horned frogs (Anura, Ceratophryidae). Journal of Systematic Palaeontology 19(2): 91–130. https://doi.org/10.1080/14772019.2021.1892845

Haddoumi H, Allain R, Meslouh S, Metais G, Monbaron M, Pons D, Rage J-C, Vullo R, Zouhri S, Gheerbrant E (2016) Guelb el Ahmar (Bathonian, Anoual Syncline, eastern Morocco): First continental flora and fauna including mammals from the Middle Jurassic of Africa. Gondwana Research 29: 290–319. https://doi.org/10.1016/j.gr.2014.12.004

Hecht MK (1963) A reevaluation of the early history of the frogs. Part II. Systematic Zoology 12: 20–35. https://doi.org/10.2307/2411892

Heinrich W-D (2003) Expeditionen in die Erdgeschichte Ostafrikas: Die Dinosaurierlagerstätte Tendaguru in Tansania. Sitzungsberichte der Gesellschaft Naturforschender Freunde zu Berlin (N. F.) 42: 5–30.

Heinrich W-D, Bussert R, Aberhan M, Hampe O, Kapilima S, Schrank E, Schultka S, Maier G, Msaky E, Sames B, Chami R (2001) The German-Tanzanian Tendaguru Expedition 2000. Mitteilungen aus dem Museum für Naturkunde in Berlin, Geowissenschaftliche Reihe 4: 223–237. https://doi.org/10.1002/mmng.4860040113

Hennig W (1914) Die Fischreste unter den Funden der Tendaguru-Expedition. Archiv für Biontologie 3: 293–312.

Holman JA (2003) Fossil frogs and toads of North America. Indiana University Press (Bloomington, USA).

Hübner TR, Foth C, Heinrich W-D, Schwarz D, Bussert R (2021) Research history, taphonomy, and age structure of a mass accumulation of the ornithopod dinosaur *Dysalotosaurus lettowvorbecki* from the Upper Jurassic of Tanzania. Acta Palaeontologica Polonica 66(2): 275–300. https://doi.org/10.4202/app.00687.2019

Janensch W (1914) Die Gliederung der Tendaguru-Schichten im Tendaguru-Gebiet und die Entstehung der Saurierlagerstätten. Archiv für Biontologie 3(3): 227–261.

Janensch W (1920) Über *Elaphrosaurus bambergi* und die Megalosaurier aus den Tendaguru-Schichten Deutsch-Ostafrikas. Sitzungsberichte der Gesellschaft naturforschender Freunde Berlin 1920: 225–235.

Janensch W (1935) Die Schädel der Sauropoden *Brachiosaurus*, *Barosaururus* und *Dicraeosaurus* aus den Tendguru-Schichten Deutsch-Ostafrikas. Palaeontographica, Supplement VII, 1. Reihe, Teil 2, Lieferung 1: 145–248.

Janensch W (1955) Der Ornithopode *Dysalotosaurus* der Tendaguru-Schichten. Palaeontographica, Supplement VII, 1. Reihe, Teil 3, Lieferung 3: 105–176.

Jenkins Jr FA, Walsh DM (1993) An Early Jurassic caecilian with limbs. Nature 365: 246–250. https://doi.org/10.1038/365246a0

Jenkins Jr FA, Walsh DM, Carroll RL (2007) Anatomy of *Eocaecilia macropodia*, a limbed caecilian of the Early Jurassic. Bulletin of the Museum of Comparative Zoology 158(6): 285–365. https://doi.org/10.3099/0027-4100(2007)158[285:AOEMAL]2.0.CO;2

Jetz W, Pyron AR (2018) The interplay of past diversification and evolutionary isolation with present imperilment across the amphibian tree of life. Nature Ecology & Evolution 2(5): 850–858. https://doi.org/10.1038/s41559-018-0515-5

Jia J, Gao K-Q (2016a) A new hynobiid-like salamander (Amphibia, Urodela) from Inner Mongolia, China, provides a rare case study of developmental features in an Early Cretaceous fossil urodele. PeerJ 4: e2499. https://doi.org/10.7717/peerj.2499

Jia J, Gao K-Q (2016b) A new basal salamandroid (Amphibia, Urodela) from the late Jurassic of Qinglong, Hebei Province, China. PLoS ONE 11: e0153834. https://doi.org/10.1371/journal.pone.0153834

Jia J, Gao K-Q (2019) A new stem hynobiid salamander (Urodela, Cryptobranchoidea) from the Upper Jurassic (Oxfordian) of Liaoning Province, China. Journal of Vertebrate Paleontology 39(2): e1588285. https://doi.org/10.1080/02724634.2019.1588285

Jia J, Anderson JS, Gao K-Q (2021) Middle Jurassic stem hynobiids from China shed light on the evolution of basal salamanders. iScience 24(7): 102744. https://doi.org/10.1016/j.isci.2021.102744

Jones MEH, Evans SE, Sigogneau-Russell D (2003) Early Cretaceous frogs from Morocco. Annals of Carnegie Museum 72: 65–99. https://doi.org/10.5962/p.215089

Jones MEH, Benson RBJ, Skutschas PP, Hill L, Panciroli E, Schmitt AD, Walsh SA, Evans SE (2022) Middle Jurassic fossils document an early stage in salamander evolution. Proceedings of the National Academy of Sciences of the United States of America 119(30): e2114100119. https://doi.org/10.1073/pnas.2114100119

Kahlert E, Schultka St, Süß H (1999) Die mesophytische Flora der Saurierlagerstätte am Tendaguru. Mitteilungen aus dem Museum für Naturkunde in Berlin, Geowissenschaftliche Reihe 2: 185–199. https://doi.org/10.5194/fr-2-185-1999

Keeffe R, Blackburn DC (2020) Comparative morphology of the humerus in forward-burrowing frogs. Biological Journal of the Linnean Society 131: 291–303. https://doi.org/10.1093/biolinnean/blaa092

Lasseron M, Allain R, Gheerbrant E, Haddoumi H, Jalil J-E, Métais G, Rage J-C, Vullo R, Zouhri S (2020) New data on the microvertebrate fauna from the Upper Jurassic or lowest Cretaceous of Ksar Metlili (Anoual Syncline, eastern Morocco). Geological Magazine 157(3): 367–392. https://doi.org/10.1017/S0016756819000761

Lemierre A, Bailon S, Folie A, Laurin M (2023) A new pipid from the Cretaceous of Africa (In Beceten, Niger) and early evolution of the Pipidae. Journal of Systematic Palaeontology 21(1): 2266428. https://doi.org/10.1080/14772019.2023.2266428

Lemierre A, Bailon S, Folie A, Laurin M (2025a) New pipimorphs from the Late Cretaceous of Niger. Annales de Paléontologie 111: 102751. https://doi.org/10.1016/j.annpal.2024.102751

Lemierre A, Pickford M, Senut B, Gommery D (2025b). Anurans from the Early Miocene of Chamtwara (western Kenya), and the first fossil record for Arthroleptidae (Afrobatrachia, Ranoidea). Palaeobiodiversity and Palaeoenvironments 105: 439–457. https://doi.org/10.1007/s12549-025-00659-0

Maier G (2003) African Dinosaurs unearthed. The Tendaguru Expeditions. Indiana University Press, Bloomington, USA, 368 pp. https://doi.org/10.2307/j.ctt1zxz0sh

Mannion PD, Upchurch P, Schwarz D, Wings O (2019) Taxonomic affinities of the putative titanosaurs from the Late Jurassic Tendaguru Formation of Tanzania: phylogenetic and biogeographic implications for eusauropod dinosaur evolution. Zoological Journal of the Linnean Society 185(3): 784–909. https://doi.org/10.1093/zoolinnean/zly068

Mao F-Y, Meng J (2019) A new haramiyidan mammal from the Jurassic Yanliao Biota and comparisons with other haramiyidans. Zoological Journal of the Linnean Society 186(2): 529–552. https://doi.org/10.1093/zoolinnean/zly088

Mishra D, Msabi M, Salimu M (2022) Review on the comparative sedimentology of Late Jurassic transgressive deposits of Tendaguru Hill - Mandawa Basin (Tanzania) and Wagad Hill - Kachchh Basin (India). Journal of the Geological Society of India 98(6): 779–786. https://doi.org/10.1007/s12594-022-2068-0

Mörs T, Reguero M, Vasilyan D (2020) First fossil frog from Antarctica: implications for Eocene high latitude climate conditions and Gondwanan cosmopolitanism of Australobatrachia. Scientific Reports 10: 5051. https://doi.org/10.1038/s41598-020-61973-5

Nakamura Y, Ota H (2015) Late Pleistocene-Holocene amphibians from Okinawajima Island in the Ryukyu Archipelago, Japan: Reconfirmed faunal endemicity and the Holocene range collapse of forest-dwelling species. Palaeontologia Electronica 18: 1–26. https://doi.org/10.26879/503

Nopcsa F (1930) Notes on Stegocephalia and Amphibia. Proceedings of the Zoological Society of London 2: 979–995. https://doi.org/10.1111/j.1096-3642.1930.tb01009.x

Otero RA, Jimenez-Huidobro P, Soto-Acuña S, Yury-Yáñez RE (2014) Evidence of a giant helmeted frog (Australobatrachia,

Calyptocephalellidae) from Eocene levels of the Magallanes Basin, southernmost Chile. Journal of South American Earth Sciences 55: 133–140. https://doi.org/10.1016/j.jsames.2014.06.010

Parkinson J (1930) The dinosaur in East Africa. An account of the giant reptile beds of Tendaguru, Tanganyika Territory. H.F. & G. Witherby, London, 192 pp.

Piveteau J (1936) Une forme ancestrale des amphibiens anoures dans le Trias inférieur de Madagascar. Comptes Rendus des Séances de l'Académie des Sciences 19: 1607–1608.

Portik D, Striecher JW, Wiens JJ (2023) Frog phylogeny: A time-based calibrated, species-level tree based on hundreds of loci and 5,242 species. Molecular Phylogenetics and Evolution 188: 107907. https://doi.org/10.1016/j.ympev.2023.107907

Rage J-C (1974) Les batraciens des gisements quaternaires européens. Détermination ostéologique. Bulletin mensuel de la Société linnéenne de Lyon 43(8): 276–289. https://doi.org/10.3406/linly.1974.10136

Rage J-C (1984) Are the Ranidae (Anura, Amphibia) known prior to the Oligocene?. Amphibia-Reptilia 5(3–4): 281–288. https://doi.org/10.1163/156853884X-005-03-09

Rauhut O (2011) Theropod dinosaurs from the Late Jurassic of Tendaguru (Tanzania). Special Papers in Palaeontology 86: 195–239.

Redelstorff R, Hübner TR, Chinsamy A, Sander P (2013) Bone histology of the Stegosaur *Kentrosaurus aethiopicus* (Ornithischia: Thyreophora) from the Upper Jurassic of Tanzania. The Anatomical Record 296: 933–952. https://doi.org/10.1002/ar.22701

Rong Y-F, Vasilyan D, Dong L-P, Wang Y (2021) Revision of *Chunerpeton tianyiense* (Lissamphibia, Caudata): Is it a cryptobranchid salamander? Palaeoworld 30: 708–723. https://doi.org/10.1016/j.palwor.2020.12.001

Sanchíz B (1998) Salientia. In: Wellnhofer P (Ed.) Encyclopedia of Palaeoherpetology, 4. München: Verlag Dr. Friedrich Pfeil.

Sanchíz B, Schleich HH, Esteban M (1993) Water frogs (Ranidae) from the Oligocene of Germany. Journal of Herpetology 27(4): 486. https://doi.org/10.2307/1564847

Sames B (2008) Application of Ostracoda and Charophyta from the Late Jurassic to Early Cretaceous Tendaguru Formation at Tendaguru, Tanzania (East Africa) - Biostratigraphy, palaeobiogeography and palaeoecology. Palaeogeography, Palaeoclimatology, Palaeoecology 264: 213–229. https://doi.org/10.1016/j.palaeo.2007.03.053

Schrank E (2005) Dinoflagellate cysts ad associated aquatic palynomorphs from the Tendaguru Beds (Upper Jurassic - Lower Cretaceous) of Southeast Tanzania. Palynology 29: 49–85. https://doi.org/10.2113/29.1.49

Schrank E (2010) Pollen and spores from the Tendaguru Beds, Upper Jurassic and Lower Cretaceous of southeast Tanzania: palynostratigraphical and paleoecological implications. Palynology 34: 3–42. https://doi.org/10.1080/01916121003620106

Schudack ME (1999) Charophytes from the Middle Dinosaur Member of the Tendaguru Formation (Upper Jurassic of Tanzania). Mitteilungen aus dem Museum für Naturkunde Berlin, Geowissenschaftliche Reihe 2: 201–205. https://doi.org/10.1002/mmng.1999.4860020115

Schudack ME, Schudack U (2002) Ostracods from the Middle Dinosaur Member of the Tendaguru Formation (Upper Jurassic of Tanzania). Neues Jahrbuch für Geologie und Paläontologie, Monatshefte 2002(6): 321–336. https://doi.org/10.1127/njgpm/2002/2002/321

Shubin NH, Jenkins FA (1995) An early Jurassic jumping frog. Nature 377: 49–52. https://doi.org/10.1038/377049a0

Sigurdsen T, Bolt JR (2009) The lissamphibian humerus and elbow joint, and the origins of modern amphibians. Journal of Morphology 270: 1443–1453. https://doi.org/10.1002/jmor.10769

Sigurdsen T, Green DM, Bishop PJ (2012) Did *Triadobatrachus* jump? Morphology and evolution of the anuran forelimb in relation to locomotion in early salientians. Fieldiana Life and Earth Sciences 5: 77–89. https://doi.org/10.3158/2158-5520-5.1.77

Stremme H (1916) Über die durch Bandverknöcherung hervorgerufene proximale Verschmelzung der Mittelhand-oder Mittel Fussknochen eines Reptils. Archiv für Biontologie 4: 143–144.

Sweetman SC, Gardner JC (2013) A new albanerpetontid amphibian from the Barremian (Early Cretaceous) Wessex Formation of the Isle of Wight, southern England. Acta Palaeontologica Polonica 58(2): 295–324.

Thiéblemont D, Liégeois J-P, Fernandez-Alonso M, Ouabadi A, Le Gall B, Maury R, Jalludin M, Vidal M, Oattara Gbélé C, Tchaméni R, Michard A, Nehlig P, Rossi P, Chêne F [Eds] (2016) Geological Map of Africa at 1:10 M scale, CGMW-BRGM. ISBN: 9782917310328. https://doi.org/10.14682/2016GEOAFR [Printed map is available at CGMW (www.cgmw.org) and BRGM (www.brgm.fr)]

Wang Y (2004) A new Mesozoic caudata (*Liaoxitriton daohugouensis* sp. nov.) from Inner Mongolia, China. Chinese Science Bulletin 49: 858–860. https://doi.org/10.1007/BF02889761

Wang Y, Evans SE (2006a) A new short-bodied salamander from the Upper Jurassic/ Lower Cretaceous of China, Aca Palaeontologica Polonica 51: 127–130.

Wang Y, Evans SE (2006b) Advances in the study of fossil amphibians and squamates from China: the past fifteen years. Vertebrata PalAsiatica 44: 60–73.

Wang Y, Rose CS (2005) *Jeholotriton paradoxus* (Amphibia: Caudata) from the Lower Cretaceous of southeastern Inner Mongolia, China. Journal of Vertebrate Paleontology 25: 523–532. https://doi.org/10.1671/0272-4634(2005)025[0523:JPACFT]2.0.CO;2

Wang Y, Roček Z, Dong L (2018) A new pelobatoid frog from the lower Eocene of southern China. Palaeobiodiversity and Palaeoenvironments 98(2): 225–242. https://doi.org/10.1007/s12549-017-0304-1

Zhang G-L, Wang Y, Jones MEH, Evans SE (2009) A new Early Cretaceous salamander (*Regalerpeton wiechangensis* gen. et sp. nov.) from the Huajiying Formation volcanic rocks in West Lianoning-North Hebei by LA-ICP-MS dating. Chinese Science Bulletin 53: 3574–3584.

Supplementary material 1

Supplemental data

Authors: Alfred J. A. Lemierre, Wolf-Dieter Heinrich, David C. Blackburn

Data type: docx

Explanation note: Lists of studied specimens for comparisons, plates illustrating the different studied humeri.

Copyright notice: This dataset is made available under the Open Database License (http://opendatacommons.org/licenses/odbl/1.0). The Open Database License (ODbL) is a license agreement intended to allow users to freely share, modify, and use this Dataset while maintaining this same freedom for others, provided that the original source and author(s) are credited.

Link: https://doi.org/10.3897/fr.29.175525.suppl1